Title: Mitochondrial citrate transporters CtpA and YhmA are involved in lysine biosynthesis in the white koji fungus, *Aspergillus luchuensis* mut. *kawachii*

Running title: Mitochondrial citrate transporters of *Aspergillus*

Chihiro Kadooka[1,2], Kosuke Izumitsu[3], Masahira Onoue,[4] Kayu Okutsu[2], Yumiko Yoshizaki[2], Kazunori Takamine[2], Masatoshi Goto[5], Hisanori Tamaki[2], Taiki Futagami[2]*

[1] United Graduate School of Agricultural Sciences, Kagoshima University, 1-21-24 Korimoto, Kagoshima, 890-0065, Japan

[2] Education and Research Center for Fermentation Studies, Faculty of Agriculture, Kagoshima University, 1-21-24 Korimoto, Kagoshima, 890-0065, Japan

[3] School of Environmental Science, University of Shiga Prefecture, 2500 Hassaka-cho, Hikone, Shiga 522-8533, Japan

[4] Research Support Center, Institute for Research Promotion, Kagoshima University, 1-21-24 Korimoto, Kagoshima, 890-0065, Japan

[5] Faculty of Agriculture, Saga University, 1 Honjo-machi, Saga, 840-8502, Japan

*Corresponding author

Tel and Fax: 81-99-285-3536

Email: futagami@chem.agri.kagoshima-u.ac.jp

ABSTRACT

Aspergillus luchuensis mut. *kawachii* produces a large amount of citric acid during the process of fermenting shochu, a traditional Japanese distilled spirit. In this study, we characterized *A. kawachii* CtpA and YhmA, which are homologous to the yeast *Saccharomyces cerevisiae* mitochondrial citrate transporters Ctp1 and Yhm2, respectively. CtpA and YhmA were purified from *A. kawachii* and reconstituted into liposomes. The proteoliposomes exhibited only counter-exchange transport activity; CtpA transported citrate using counter substrates especially for *cis*-aconitate and malate, whereas YhmA transported citrate using a wider variety of counter substrates, including citrate, 2-oxoglutarate, malate, *cis*-aconitate, and succinate. Disruption of *ctpA* and *yhmA* caused deficient hyphal growth and conidia formation with reduced mycelial weight–normalized citrate production. Because we could not obtain a Δ*ctpA* Δ*yhmA* strain, we constructed a *ctpA-S* conditional expression strain in the Δ*yhmA* background using the Tet-On promoter system. Knockdown of *ctpA-S* in Δ*yhmA* resulted in a severe growth defect on minimal medium, indicating that double disruption of *ctpA* and *yhmA* leads to synthetic lethality; however, we subsequently found that the severe growth defect was relieved by addition of lysine. Our results indicate that CtpA and YhmA are mitochondrial citrate transporters involved in citric acid production and that transport of citrate from mitochondria to the cytosol plays an important role in lysine biogenesis in *A. kawachii*.

IMPORTANCE

Citrate transport is believed to play a significant role in citrate production by filamentous fungi; however, details of the process remain unclear. This study characterized two citrate transporters from *Aspergillus luchuensis* mut. *kawachii*.

Biochemical and gene disruption analyses showed that CtpA and YhmA are mitochondrial citrate transporters required for normal hyphal growth, conidia formation, and citric acid production. In addition, this study provided insights into the links between citrate transport and lysine biosynthesis. The characteristics of fungal citrate transporters elucidated in this study will help expand our understanding of the citrate production mechanism and facilitate the development and optimization of industrial organic acid fermentation processes.

KEYEORDS

Aspergillus luchuensis mut. *kawachii*, shochu, citrate transporter, CtpA, YhmA, lysine biosynthesis

INTRODUCTION

The white koji fungus, *Aspergillus luchuensis* mut. *kawachii* (*A. kawachii*), is a filamentous fungus used for the production of shochu, a traditional Japanese distilled spirit (1, 2). During the shochu fermentation process, *A. kawachii* secretes large amounts of the glycoside hydrolases α-amylase and glucoamylase, which degrade starches contained in cereal ingredients such as rice, barley, and sweet potato (3). The resulting monosaccharides or disaccharides can be further utilized by the yeast *Saccharomyces cerevisiae* for ethanol fermentation. In addition to this feature, *A. kawachii* produces a large amount of citric acid, which lowers the pH of the "*moromi*" (mash) to between 3 and 3.5, thereby preventing the growth of contaminant microbes. This feature is important because shochu is mainly produced in relatively warm areas of Japan, such as Kyushu and Okinawa islands.

Although a clearly different species, *A. kawachii* is phylogenetically closely related to *Aspergillus niger*, which is commonly used in the citric acid fermentation industry (4-6). The mechanism of citric acid production by *A. niger* has been investigated from various perspectives, and related metabolic pathways have been elucidated (7-9). Carbon sources such as glucose and sucrose are metabolized to produce pyruvate via the glycolytic pathway; subsequently, citric acid is synthesized by citrate synthase as an intermediate compound of the tricarboxylic acid cycle in mitochondria and excreted to the cytosol prior to subsequent excretion to the extracellular environment. A previous study detected citrate synthase activity primarily in the mitochondrial fraction (10). Experiments involving overexpression of the citrate synthase–encoding *citA* gene indicated that citrate synthase plays only a minor role in controlling the flux of the pathway involved in citric acid production (11). By contrast, a mathematical analysis suggested that citric acid overflow might be controlled by the transport process (e.g.,

uptake of carbon source, pyruvate transport from the cytosol to mitochondria, transport of citrate from mitochondria to the cytosol and then extracellular excretion) (12-14).

Mitochondrial citrate transporters of mammals and *S. cerevisiae* have been well characterized. Biochemical studies revealed that rat liver citrate transporter (CTP) catalyzes the antiport reaction of the dibasic form of tricarboxylic acids (e.g., citrate, isocitrate, and *cis*-aconitate) with other tricarboxylic acids, dicarboxylic acids (e.g., malate, succinate, maleate), or phosphoenolpyruvate (15-17), whereas the *S. cerevisiae* citrate transporter (Ctp1) shows stricter substrate specificity for tricarboxylic acids compared with CTP (18, 19). Cytosolic citrate is used in the production of acetyl-CoA, which plays a significant role in the biosynthesis of fatty acids and sterols in mammalian cells (20-23). However, no phenotypic changes were observed in *S. cerevisiae* following disruption of the *CTP1* gene (24), perhaps because other transport processes (e.g., involving mitochondrial succinate/fumarate transporter Acr1) control acetyl-CoA synthesis (25-27). A homolog to the *CTP1* gene (*ctpA*) was recently characterized in *A. niger*, with a focus on the relationship between citrate transport and the organism's high citrate production capability (28). Disruption of the *ctpA* gene led to reduced growth and citric acid production in *A. niger* only during the early logarithmic phase, indicating that CtpA is not a major mitochondrial citrate transporter in *A. niger* (28).

To better understand the mechanism of citric acid production by *A. kawachii*, we previously characterized the changes in gene expression that occur during solid-state culture, which is used for brewing shochu (29). During the shochu-making process, the cultivation temperature is tightly controlled, with gradual increase to 40°C and then lowering to 30°C. Lowering of the temperature is required to enhance production of citric acid (30). We sought to identify genes related to citric acid production and

reported that expression of the gene encoding the putative mitochondrial citrate/malate transporter (AKAW_03754, CtpA) increased 1.78-fold upon lowering of the temperature (29). Subsequently, we found that expression of a putative mitochondrial citrate transporter (AKAW_06280, YhmA) gene, which is a homolog of the mitochondrial citrate/2-oxoglutarate transporter Yhm2 of *S. cerevisiae* (31), increased 1.76-fold, based on analysis of a microarray dataset (29). Yhm2 of *S. cerevisiae* was first characterized as a DNA-binding protein predicted to play a role in replication and segregation of the mitochondrial genome (32). However, subsequent biochemical and genetic studies revealed that Yhm2 is a mitochondrial transporter that catalyzes the antiport reaction of citrate and 2-oxoglutarate (31). Yhm2 also exhibited transporter activity for oxaloacetate, succinate, and to a lesser extent, fumarate. Yhm2 plays a significant physiologic role in the citrate/2-oxoglutarate NADPH redox shuttle in *S. cerevisiae* to reduce levels of reactive oxygen species.

In this study, we focused on characterizing both CtpA and YhmA of *A. kawachii* to uncover the functional role of these putative mitochondrial citrate transporters. Our biochemical analyses of purified CtpA and YhmA and phenotypic analyses of disruptant strains confirmed that CtpA and YhmA are mitochondrial citrate carriers involved in citric acid production. Our findings also suggest that double disruption of *ctpA* and *yhmA* induces a synthetic lethal phenotype in minimal (M) medium and that the process of transporting citrate from mitochondria to the cytosol is of physiologic significance for lysine biosynthesis in *A. kawachii*.

RESULTS

Sequence features of CtpA and YhmA. The *A. kawachii* genes *ctpA* and *yhmA* encode proteins of 296 and 299 amino acid residues, respectively. These proteins were

found to contain six predicted transmembrane domains and three P-X-(D/E)-X-X-(R/K) sequences, which are common characteristics of mitochondrial carrier proteins (33-35) (Fig. S1 in the supplemental material).

Amino acid sequence identities of 47, 35, and 71% were determined between *A. kawachii* CtpA and *S. cerevisiae* Ctp1, between *A. kawachii* CtpA and rat CTP, and between *A. kawachii* YhmA and *S. cerevisiae* Yhm2, respectively. The amino acid residues required for interacting with citrate in *S. cerevisiae* Ctp1 (site I [K83, R87, and R189] and site II [K37, R181, K239, R276, and R279]) were conserved in *A. kawachii* CtpA (36, 37) (Fig. S1A in the supplemental material). The predicted substrate binding sites in *S. cerevisiae* Yhm2 (site I [E83, K87, and L91], site II [R181 and Q182], and site III [R279]) were also conserved in *A. kawachii* YhmA (31, 35) (Fig. S1B in the supplemental material).

The *A. kawachii* genome contained an additional *S. cerevisiae yhm2* homologous gene, *yhmB* (AKAW_02589) (Fig. S1B in the supplemental material), which encodes a protein of 309 amino acid resides with a 53% sequence identity to Yhm2. All of the amino acid residues of sites I, II, and III in Yhm2 mentioned above were found to be conserved in YhmB, suggesting that YhmB functions as a mitochondrial carrier protein. However, no *yhmB* transcripts were detected in microarray analyses during the shochu fermentation process (29). In addition, disruption of *yhmB* did not induce a phenotypic change in *A. kawachii* in M medium (data not shown). Thus, we excluded analysis of the *yhmB* gene from this study.

Transport activity of CtpA and YhmA. To clarify whether CtpA and YhmA are citrate transporters, we purified the proteins and assayed their activity. For the purification of CtpA and YhmA, C-terminal S-tag fusion proteins were expressed in *A. kawachii* Δ*ctpA* and Δ*yhmA* strains, respectively, under control of the Tet-On promoter,

and the products were purified using S-protein agarose (Fig. S2 in the supplemental material). Purified CtpA and YhmA were reconstituted into liposomes using a freeze/thaw sonication procedure, and then [^{14}C]-citrate uptake into proteoliposomes was assessed as either uniport (absence of internal substrate) or antiport (presence of internal substrate such as oxaloacetate, succinate, *cis*-aconitate, citrate, 2-oxoglutarate, or malate). Uptake of [^{14}C]-citrate was only observed under antiport conditions for both CtpA and YhmA reconstituted proteoliposomes (Fig. 1A and B). CtpA exhibited higher specificity for *cis*-aconitate and malate and showed activity in the presence of oxaloacetate, succinate, and citrate, although to a lesser extent (Fig. 1A). Much lower activity of CtpA was also detected in the presence of 2-oxoglutarate. By contrast, YhmA exhibited wider specificity, with activity toward citrate, 2-oxoglutarate, malate, *cis*-aconitate, and succinate to the same extent and activity in the presence of oxaloacetate to a lesser extent (Fig. 1B).

Phenotype of control, Δ*ctpA*, Δ*yhmA*, and Ptet-*ctpA*-*S* Δ*yhmA* strains. To explore the physiologic roles of CtpA and YhmA, we characterized the colony morphology of the *A. kawachii* Δ*ctpA* and Δ*yhmA* strains. The Δ*ctpA* strain showed a growth defect at 25 and 30°C, and the defective phenotype was restored at 37 and 42°C (Fig. 2A). This result agreed with a previous report indicating that the *A. niger* Δ*ctpA* strain is more sensitive to low-temperature stress (28). By contrast, the Δ*yhmA* strain exhibited smaller colony diameter than the control strain on M medium at all temperatures tested.

Because the colonies of the Δ*ctpA* and Δ*yhmA* strains were paler in color than colonies of the control strain, we assessed conidia formation (Fig. 2B). Strains were cultivated on M medium at 30°C for 4 days, at which time the number of conidia formed was determined. The number of conidia per cm^2 of the Δ*ctpA* and Δ*yhmA* strains declined significantly, to approximately 30% of the number produced by the control

strain (Fig. 2B), indicating that CtpA and YhmA are involved in conidia formation. Complementation of *ctpA* (Δ*ctpA* + *ctpA*) and *yhmA* (Δ*yhmA* + *yhmA*) successfully reversed the above-mentioned deficient phenotypes of the Δ*ctpA* and Δ*yhmA* strains.

We then attempted to construct a *ctpA*/*yhmA* double disruptant by disrupting the *yhmA* gene in the Δ*ctpA* strain. However, all of transformants obtained were heterokaryotic gene disruptants (data not shown). Therefore, we constructed a strain that conditionally expressed the S-tagged *ctpA* gene (*ctpA-S*) using the Tet-On system and then disrupted the *yhmA* gene under *ctpA-S*–expressing conditions using doxycycline (Dox), yielding strain Ptet-*ctpA-S* Δ*yhmA*. Dox-controlled expression of CtpA-S was confirmed at the protein level by immunoblot analysis using anti–S-tag antibody (Fig. S3 in the supplemental material, right panel). The Ptet-*ctpA-S* Δ*yhmA* strain exhibited a severe growth defect in M medium without Dox (*ctpA-S* expression is not induced in the absence of Dox) (Fig. 2C), indicating that double disruption of *ctpA* and *yhmA* induces synthetic lethality in M medium.

Organic acid production by control, Δ*ctpA*, Δ*yhmA*, and Ptet-*ctpA-S* Δ*yhmA* strains. To investigate the physiologic role of CtpA and YhmA in organic acid production, we compared organic acid production by the control, Δ*ctpA*, Δ*yhmA*, and Ptet-*ctpA-S* Δ*yhmA* strains (Fig. 3). The control, Δ*ctpA*, and Δ*yhmA* strains were pre-cultivated in M medium at 30°C for 36 h and then transferred to CAP medium and further cultivated at 30°C for 48 h. By contrast, the Ptet-*ctpA-S* Δ*yhmA* strain was pre-cultured in M medium with Dox before transfer to CAP medium without Dox because this strain cannot grow in the absence of Dox (non-induced *ctpA-S* expression condition). CAP medium was used for organic acid production because it contains a high concentration of carbon source (10% [wt/vol] glucose) and appropriate trace elements (7-9). We measured organic acid levels in the culture supernatant and mycelia

separately as the extracellular and intracellular fractions, respectively.

In the extracellular fraction, citric acid was detected as the major organic acid, but malic acid and 2-oxoglutaric acid were also detected using our HPLC system (Fig. 3A). The Δ*ctpA* strain exhibited 3.0-fold greater production of extracellular 2-oxoglutaric acid compared with the control strain, whereas the Δ*yhmA* strain exhibited 0.27-fold lower citric acid and 1.7-fold greater 2-oxoglutaric acid production. In addition, the Ptet-*ctpA-S* Δ*yhmA* strain exhibited 0.047-fold lower citric acid production, 2.4-fold greater malic acid production, and 16-fold greater 2-oxoglutaric acid production in the extracellular fraction.

In the intracellular fraction, citric acid, malic acid, and 2-oxoglutaric acid were detected at similar concentrations (Fig. 3B). The decrease in production of citric acid by the Δ*ctpA* and Δ*yhmA* strains was not statistically significant, but the Δ*ctpA* strain exhibited 0.58-fold lower malic acid production, and the Δ*yhmA* strain exhibited 0.46- and 0.50-fold lower malic acid and 2-oxoglutaric acid production, respectively, compared with the control strain. By contrast, the intracellular concentrations of citric acid, malic acid, and 2-oxoglutaric acid produced by the Ptet-*ctpA-S* Δ*yhmA* strain were 0.18-, 0.18-, and 0.35-fold lower than the control, respectively.

These results indicate that CtpA and YhmA play a significant role in organic acid production in *A. kawachii*. The concentration of citric acid produced tended to be negatively correlated with the concentrations of malic acid and 2-oxogluataric acid in the extracellular fraction. In addition, the Ptet-*ctpA-S* Δ*yhmA* strain exhibited the most significant change, especially with regard to the reduced concentration of citric acid in both the extracellular and intracellular fractions, suggesting that CtpA and YhmA function redundantly in citric acid production.

Transcriptional analysis of *ctpA* and *yhmA*. To investigate the effect of growth

phase on expression of the *ctpA* and *yhmA* genes, we performed real-time reverse transcription PCR analysis using RNA extracted from mycelia and conidia of the *A. kawachii* control strain. The control strain was cultivated in M liquid medium or M agar medium for generation of mycelia or conidia, respectively. The growth phase during liquid cultivation was evaluated by measuring the weight of freeze dried mycelia (Fig. 4A). Based on mycelial weight, 0 to 24 h, 24 to 30 h, 30 to 36 h, and 36 to 60 h corresponded to the lag, early log, late log, and stationary phases, respectively. We tested the quality of conidial RNA by assessing production of *wetA* transcripts, which are abundant in dormant *A. niger* conidia (38). The level of *wetA* transcription was 13-fold higher in conidia than mycelia for culture in M liquid medium for 36 h, indicating that extraction of RNA from the conidia was successful (Fig. 4B).

We then investigated transcription of the *ctpA* and *yhmA* genes (Fig. 4C). The level of *ctpA* expression was relatively constant across the vegetative growth period, whereas expression increased significantly in conidia. By contrast, expression of *yhmA* increased significantly at 48 h (stationary phase) and then decreased at 60 h. The level of *yhmA* transcripts in the conidia was similar to that in vegetative hyphae in the lag and log phases.

We also investigated the effect of medium composition (M or CAP medium) on the transcription of *ctpA* and *yhmA* because *A. kawachii* produces a large amount of citric acid in CAP medium but not M medium (Fig. 4D). Expression levels of both *ctpA* and *yhmA* were higher in CAP medium than M medium.

Subcellular localization of CtpA and YhmA. To determine the subcellular localization of CtpA and YhmA, green fluorescent protein (GFP) was fused to the C-terminus of CtpA and YhmA and expressed in the Δ*ctpA* and Δ*yhmA* strains, respectively, under control of the respective native promoters. Functional expression of

CtpA-GFP and YhmA-GFP was confirmed by complementation of the deficient phenotype of the Δ*ctpA* and Δ*yhmA* strains (Fig. 5A). We first examined the strains expressing CtpA-GFP and YhmA-GFP when grown in M medium. Green fluorescence associated with YhmA-GFP merged well with the red fluorescence of MitoTracker Red CMXRos, which stains mitochondria (Fig. 5B). No green fluorescence was detected for the strain expressing CtpA-GFP in M medium, however (data not shown). Because the *ctpA* and *yhmA* genes were transcribed at higher levels in CAP medium than M medium (Fig. 4D), we then cultivated the strains in CAP medium. Green fluorescence associated with YhmA-GFP (Fig. 5C, left panel) and CtpA-GFP (Fig. 5C right panel) was detected, and this fluorescence merged with the red fluorescence, although not completely. This result suggests that CtpA-GFP and YhmA-GFP are localized in the mitochondria, but this should be confirmed through additional experiments.

Immunoblot analysis using an anti-GFP antibody indicated that CtpA-GFP and YhmA-GFP were expressed at their predicted molecular weights (59.8 kDa and 61.1 kDa, respectively) (Fig. S4 in the supplemental material). In addition, the bands for both CtpA-GFP and YhmA-GFP exhibited greater intensity with cultivation in CAP medium than M medium, indicating that conditions favorable for citric acid production enhance expression of *ctpA* and *yhmA* at both the mRNA (Fig. 4D) and protein levels.

Complementation test of *ctpA* and *yhmA* in *S. cerevisiae* strains Δ*ctp1* and Δ*yhm2*. To determine whether *A. kawachii ctpA* and *yhmA* can complement the defect in *S. cerevisiae* strains Δ*ctp1* and Δ*yhm2*, the *ctpA* and *yhmA* genes were expressed in *S. cerevisiae* Δ*ctp1* and Δ*yhm2*, respectively, under control of the respective native promoters.

We first characterized the phenotype of the *S. cerevisiae* Δ*ctp1* strain, because no phenotypic change was observed following disruption of *ctp1* (24). We performed a spot

growth assay under cultivation conditions including low temperature stress at 15°C, cell wall stress (Congo red and calcofluor white), and varying carbon source (glucose, acetate, or glycerol). However, as no phenotypic changes were observed following disruption of *ctp1* (data not shown), complementation testing was not possible for *ctpA*.

The *S. cerevisiae* Δ*yhm2* strain reportedly exhibits a growth defect in acetate (SA) medium but not in glucose (SD) medium (Fig. 6) (31). Complementation of *yhmA* (Δ*yhm2* + *yhmA*) remedied the deficient growth of the Δ*yhm2* strain in SA medium as well as the positive control vector carrying *YHM2* (Δ*yhm2* + *YHM2*), indicating that *yhmA* complements the loss of *YHM2* function in *S. cerevisiae*.

Intracellular levels of nicotinamide cofactors. It was hypothesized that one physiologic role of Yhm2 in *S. cerevisiae* is to increase the NADPH level in the cytosol (31). Thus, we investigated the effect of disrupting *ctpA* and *yhmA* on the intracellular redox state of *A. kawachii*. The control, Δ*ctpA*, and Δ*yhmA* strains were pre-cultivated in M medium at 30°C for 36 h and then transferred to CAP medium and further cultivated at 30°C for 12 h, at which time the NADH/ NAD^+ ratio, total amount of NADH and NAD^+, NADPH/$NADP^+$ ratio, and total amount of NADPH and $NADP^+$ were determined (Table 1).

No significant changes were observed with respect to the intracellular NADH/NAD^+ ratio and total amount of NADH and NAD^+ in the Δ*ctpA* and Δ*yhmA* strains compared with the control strain. However, the intracellular NADPH/$NADP^+$ ratio in the Δ*yhmA* strain was significantly lower than that in the control strain, though there was no significant difference in the total amount of NADPH and $NADP^+$ between the Δ*yhmA* strain and the control strain, indicating that the NADPH level was reduced in the Δ*yhmA* strain compared with the control strain. By contrast, the NADPH/$NADP^+$ ratio and total amount of NADPH and $NADP^+$ did not significantly differ between the Δ*ctpA* strain and

the control strain. This result was consistent with a previous report indicating a reduced NADPH/$NADP^+$ ratio in the cytosol of the *S. cerevisiae* Δ*yhm2* strain but not in the cytosol of the Δ*ctp1* strain (31).

Intracellular amino acid levels. Citric acid cycle intermediates are known to serve as substrates for amino acid synthesis in eukaryotic cells (39). Thus, we investigated whether disruption of *ctpA* and *yhmA* affects the intracellular amino acid levels. To compare the intracellular concentrations of amino acids, *A. kawachii* control, Δ*ctpA*, Δ*yhmA*, and Ptet-*ctpA*-*S* Δ*yhmA* strains were pre-cultivated in M medium at 30°C for 36 h and then transferred to CAP medium and further cultivated at 30°C for 48 h, at which time amino acid levels in the intracellular fraction were determined.

The intracellular concentration of lysine was significantly lower (0.31- and 0.41-fold) in the Δ*ctpA* and Δ*yhmA* strains, respectively, compared with the control strain (Table 2). Furthermore, the Ptet-*ctpA*-*S* Δ*yhmA* strain exhibited decreased concentrations of versatile amino acids, including aspartic acid, tyrosine, valine, glutamic acid, glycine, histidine, lysine, and alanine (0.43-, 0.19-, 0.32-, 0.43-, 0.35-, 0.51-, 0.22-, and 0.25-fold reduction, respectively).

Effect of amino acids on growth of the Ptet-*ctpA*-*S* Δ*yhmA* strain. Because we found that disruption of *ctpA* and *yhmA* significantly reduced the concentrations of intracellular amino acids (Table 2), we investigated whether the severe growth defect of the Ptet-*ctpA*-*S* Δ*yhmA* strain in M medium without Dox (Fig. 2C) is due to a defect in amino acid synthesis. The Ptet-*ctpA*-*S* Δ*yhmA* strain was cultivated in M medium with or without Dox or with various amino acids at a concentration of 0.5% (wt/vol) (Fig. 7A). The defective growth of the Ptet-*ctpA*-*S* Δ*yhmA* strain was not remedied by supplementation with proline or histidine, but the defect was remedied to some extent by supplementation with aspartic acid, phenylalanine, arginine, and glutamic acid and

significantly remedied by supplementation with lysine. Thus, we further examined the effect of lysine at concentrations ranging from 0.2 to 27 mM (27 mM corresponds to 0.5% [wt/vol]). The results confirmed that addition of lysine remedies the growth defect of the Ptet-*ctpA-S* Δ*yhmA* strain in M medium without Dox (Fig. 7B). Together with the intracellular amino acid level data, this result indicates that CtpA and YhmA are required for lysine biosynthesis and that a lack of lysine causes a significant growth defect in the Ptet-*ctpA-S* Δ*yhmA* strain.

DISCUSSION

In this study, we attempted to identify the mitochondrial citrate transporters in the citric acid–producing fungus, *A. kawachii*. We identified two candidates, CtpA and YhmA, as mitochondrial citrate transporters in *A. kawachii* based on sequence homology to *S. cerevisiae* Ctp1 and Yhm2, respectively (24, 31). The homologs of Ctp1 are conserved in higher eukaryotes, whereas the homologs of Yhm2 are not conserved in higher eukaryotes such as mammals (31). Interestingly, we found that the *yhmA* gene is conserved downstream of the citrate synthase–encoding gene *citA* in members of the Pezizomycotina, a subphylum of the Ascomycota (Table S1 in the supplemental material). In addition, an RNA-binding protein–encoding gene that is a homolog of *NRD1* in *S. cerevisiae* (40) that localizes upstream of the *citA* gene is also conserved. This gene cluster seems to be conserved in the Pezizomycotina but not in other subdivisions of the Ascomycota, Saccharomycotina (including *S. cerevisiae*), and Taphrinomycotina. Thus, the gene cluster might have arisen during evolution of the Pezizomycotina.

A previous investigation of an *A. niger ctpA* deletion mutant showed that *ctpA* is involved in citric acid production during the early growth stage (28); however, whether

this gene was involved in citrate transport remained unclear. Our biochemical experiments confirmed that CtpA and YhmA of *A. kawachii* are citrate transporters. YhmA and CtpA reconstituted proteoliposomes exhibited only counter-exchange transport activity, as previously reported for Ctp1 and Yhm2 (24, 31).

CtpA exhibited citrate transport activity using counter substrates, particularly *cis*-aconitate and malate (Fig. 1A). The substrate specificity of CtpA was very similar to that of yeast Ctp1 and rat CTP, known citrate/malate carriers (18, 37), except that CtpA also exhibited relatively low citrate/citrate exchange activity, unlike Ctp1 and CTP (15, 18, 41). YhmA exhibited citrate transport activity using a wider variety of counter substrates, including citrate, 2-oxoglutarate, malate, *cis*-aconitate, and succinate (Fig. 1B). The substrate specificity of YhmA was also similar to that of Yhm2, with some exceptions (31). Malate and *cis*-aconitate were identified as low-specificity substrates for Yhm2 (31), whereas YhmA exhibited relatively high specificity for malate and *cis*-aconitate.

In analyses of intracellular organic acids, we detected citrate, malate, and 2-oxoglutarate at similar levels of approximately 10 μmol/g wet mycelial weight in the control strain (specifically, citrate: 8.24 μmol/g wet mycelia, malate: 11.07 μmol/g wet mycelia, 2-oxoglutarate: 16.93 μmol/g wet mycelia) (Fig. 3B). Thus, these organic acids appear to be present at comparable concentrations in *A. kawachii* cells. The finding that purified CtpA exhibited higher citrate transport activity when malate was used as the counter substrate, compared with 2-oxoglutarate, suggests that CtpA functions primarily as a citrate/malate carrier *in vivo* (Fig. 8). Purified YhmA exhibited almost equal citrate transport activity when malate or 2-oxoglutarete was used as the counter substrate, suggesting that both malate and 2-oxoglutarate might be physiologic substrates for citrate transport by YhmA.

385 The *A. kawachii yhmA* gene complemented the defective phenotype of the *S.*
386 *cerevisiae* Δ*yhm2* strain (Fig. 6). Also, disruption of *yhmA* caused a reduction in the
387 NADPH/$NADP^+$ ratio, as previously reported in a study of the *S. cerevisiae* Δ*yhm2*
388 strain (Table 1) (31). These results suggest that YhmA plays a role in increasing the
389 NADPH reducing power in the cytosol of *A. kawachii*, similar to *S. cerevisiae* Yhm2
390 (31). According to metabolic models of *S. cerevisiae* (31) and *A. niger* (42), cytosolic
391 citrate could be converted to 2-oxoglutarate via isocitrate by cytosolic aconitase
392 (AKAW_02593 and AKAW_06497) and $NADP^+$-dependent isocitrate dehydrogenase
393 (AKAW_02496) (Fig. 8). During this reaction, $NADP^+$ is converted to NADPH by
394 $NADP^+$-dependent isocitrate dehydrogenase.

395 We could not construct a *ctpA* and *yhmA* double disruptant. In addition,
396 downregulation of *ctpA-S* in the Ptet-*ctpA-S* Δ*yhmA* strain caused a severe growth
397 defect in M medium (Fig. 2C). These results indicate that double disruption of *ctpA* and
398 *yhmA* causes synthetic lethality in M medium. Disruption of *ctpA* and/or *yhmA* caused a
399 significant reduction in the intracellular lysine concentration (Table 2), and we found
400 that supplementation with lysine relieved the growth defect of the Ptet-*ctpA-S* Δ*yhmA*
401 strain in M medium without Dox (Fig. 7A and B). In fungi, lysine is synthesized from
402 cytosolic 2-oxoglutarate via the α-aminoadipate pathway (43-48). The 2-oxoglutarate
403 available for lysine biosynthesis might be derived primarily from citrate transported by
404 CtpA and YhmA in *A. kawachii* through the metabolic pathway described above (Fig.
405 8).

406 The lysine auxotrophic phenotype of the *A. kawachii* Ptet-*ctpA* Δ*yhmA* strain was
407 inconsistent with a previous report indicating that the phenotype of the *S. cerevisiae*
408 Δ*ctp1* Δ*yhm2* strain is very similar to that of the Δ*yhm2* strain (31). Because the prior
409 study used a *lys2*-801 genetic background strain of *S. cerevisiae* (31), the strains were

cultivated in medium supplemented with lysine. Thus, we constructed a *ctp1* and *yhm2* double disruptant using *S. cerevisiae* strain W303-1A carrying the *LYS2* gene to clarify whether double disruption of *ctp1* and *yhm2* results in a lysine auxotrophic phenotype in *S. cerevisiae*. However, the Δ*ctp1* Δ*yhm2* strain carrying *LYS2* exhibited a phenotype similar to that of the previously reported Δ*ctp1* Δ*yhm2 lys2*-801 strain (31) (data not shown). Thus, citrate transporters appear to have different physiologic roles in *A. kawachii* and *S. cerevisiae* with respect to lysine biosynthesis. In addition, it was recently reported that the mitochondrial carriers Yhm2, Odc1, and Odc2 are essential for lysine and glutamate biosynthesis in *S. cerevisiae* (49). Because Odc1 and Odc2 function primarily in transporting 2-oxoadipate and 2-oxoglutarate from the mitochondria to the cytosol (50), these 2-oxodicarboxylates are thought to be involved in lysine and glutamate biosynthesis, respectively (49). An Odc1 and Odc2 homolog-encoding gene (AKAW_05597) is present in the genome of *A. kawachii*. Therefore, the physiologic role of this protein in lysine biosynthesis should be further studied to clarify the different roles of mitochondrial transporters in *A. kawachii* and *S. cerevisiae*.

In conclusion, CtpA and YhmA are mitochondrial citrate transporters involved in citric acid production and lysine biosynthesis in *A. kawachii*. *Aspergillus kawachii* is widely used in the shochu fermentation industry in Japan. Thus, our findings are expected to enhance understanding of the citric acid production mechanism and facilitate optimization of strategies to control the activity of *A. kawachii*.

MATERIALS AND METHODS

Strains and culture conditions. *Aspergillus kawachii* strain SO2 (51) and *S. cerevisiae* strain W303-1A (52) were used as parental strains in this study (Table S2).

435 Control *A. kawachii* and *S. cerevisiae* strains were defined to show same auxotrophic
436 background for comparison with the respective disruption and complementation strains.

437 *Aspergillus kawachii* strains were cultivated in M medium (53, Fungal Genetics
438 Stock Center [FGSC] [http://www.fgsc.net/methods/anidmed.html]) with or without
439 0.211% (wt/vol) arginine and/or 0.15% (wt/vol) methionine or CAP (citric acid
440 production) medium (10% [wt/vol] glucose, 0.3% [wt/vol] $(NH_4)_2SO_4$, 0.001% [wt/vol]
441 KH_2PO_4, 0.05% [wt/vol] $MgSO_4 \cdot 7H_2O$, 0.000005% [wt/vol] $FeSO_4 \cdot 7H_2O$, 0.00025%
442 [wt/vol] $ZnSO_4 \cdot 5H_2O$, 0.00006% [wt/vol] $CuSO_4 \cdot 5H_2O$ [pH 4.0]). CAP medium was
443 adjusted to the required pH with HCl.

444 *Saccharomyces cerevisiae* strains were grown in YPD medium, synthetic complete
445 (SC) medium, or minimal medium containing 2% (wt/vol) glucose (SD) or 1% (wt/vol)
446 sodium acetate (SA) as a carbon source (54).

447 **Construction of *ctpA* and *yhmA* disruptants.** The *ctpA* and *yhmA* genes were
448 disrupted by insertion of the *argB* gene. The gene disruption cassette encompassing 2 kb
449 of the 5'-end of the target gene, 1.8 kb of *argB*, and 2 kb of the 3'-end of the target gene
450 was constructed by recombinant PCR using the primer pairs
451 AKxxxx-FC/AKxxxx-del-R1, AKxxxx-F2/AKxxxx-R2, and
452 AKxxxx-del-F3/AKxxxx-RC, respectively (where 'xxxx' indicates ctpA or yhmA;
453 Table S3 in the supplemental material). For amplification of the *argB* gene, the plasmid
454 pDC1 was used as template DNA (55). The resultant DNA fragment was amplified with
455 the primers AKxxxx-F1 and AKxxxx-R3 and used to transform *A. kawachii* strain SO2,
456 yielding the Δ*ctpA* and Δ*yhmA* strains. Transformants were selected on M agar medium
457 without arginine. Introduction of the *argB* gene into the target locus was confirmed
458 based on PCR using the primer pairs AKxxxx-FC and AKxxxx-RC and the SalI
459 digestion pattern (Fig. S5A and B in the supplemental material). After the confirmation

of gene disruption, the Δ*ctpA* and Δ*yhmA* strains were transformed with the *sC* gene cassette to use the same auxotrophic genetic background strains for the comparative study. The *sC* gene cassette was prepared by PCR using *A. kawachii* genomic DNA as template DNA and the primer pair sC-comp-F and sC-comp-R (Table S3 in the supplemental material). Transformants were selected on M agar medium without methionine.

Construction of complementation strains for the *ctpA* and *yhmA* disruptants. To analyze complementation of the *ctpA* and *yhmA* disruptants with wild type (wt) *ctpA* and *yhmA*, respectively, gene replacement cassettes encompassing 2 kb of the 5'-end of the target gene, 1.4 kb of wt *ctpA* or *yhmA*, 4.2 kb of *sC*, and 1.8 kb of *argB* were constructed by recombinant PCR using the primer pairs AKxxxx-FC/AKxxxx-comp-R1 and AKxxxx-comp-F2/AKxxxx-comp-R2 (where 'xxxx' indicates *ctpA* or *yhmA*; Table S3 in the supplemental material). Fragments totaling 6 kb of *sC* and *argB* were simultaneously amplified using a plasmid carrying tandemly connected *sC* and *argB* as the template. Transformants were selected on M agar medium without methionine. Introduction of the wt *ctpA* gene into the *ctpA* disruptant was confirmed by PCR using the primer pairs AKctpA-FC/AKctpA-comp-R2 and AKctpA-comp-F2/AKctpA-comp-R2 (Fig. S5C in the supplemental material). Introduction of the wt *yhmA* gene into the *yhmA* disruptant was confirmed by PCR using the primer pair AKyhmA-FC and AKyhmA-RC (Fig. S5D in the supplemental material).

Construction of strains expressing CtpA-S and YhmA-S. The pVG2.2 vector (56) was obtained from the FGSC (Manhattan, KS) and used to construct *A. kawachii* strains expressing S-tag–fused CtpA or YhmA under control of the Tet-On promoter. First, the *pyrG* marker gene of pVG2.2 was replaced with the *sC* marker gene. The *sC*

gene was amplified by PCR using *A. nidulans* genomic DNA as the template and the primers pVG2.2ANsC-inf-F1 and pVG2.2ANsC-inf-R1 (Table S3 in the supplemental material). The resulting PCR amplicon was cloned into pVG2.2 digested with AscI. Second, the intergenic regions of AKAW_01302 and AKAW_01303 were cloned into the vector for integration into the locus of the *A. kawachii* genome. The intergenic regions of AKAW_01302 and AKAW_01303 were amplified by PCR using *A. kawachii* genomic DNA and the primers pVG2.2ANsC-inf-F2 and pVG2.2ANsC-inf-R2. The resulting PCR amplicons were cloned into the vector digested with PmeI, yielding pVG2.2ANsC.

Next, the *yhmA-S* and *ctpA-S* genes were amplified by PCR using the primer sets pVG2.2ANsC-yhmA-S-inf-F/pVG2.2ANsC-yhmA-S-inf-R and pVG2.2ANsC-ctpA-S-inf-F/pVG2.2ANsC-ctpA-S-inf-R, respectively. The amplified fragments were cloned into the PmeI site of pVG2.2ANsC, yielding pVG2.2ANsC-ctpA-S and pVG2.2ANsC-yhmA-S, respectively. An In-Fusion HD cloning kit (Takara Bio, Shiga, Japan) was used for cloning reactions.

Finally, pVG2.2ANsC-ctpA-S and pVG2.2ANsC-yhmA-S were used to transform the Δ*ctpA* and Δ*yhmA* strains, yielding strains Ptet-*ctpA-S* and Ptet-*yhmA-S*, respectively. Transformants were selected on M agar medium without methionine. Dox-controlled conditional expression of CtpA-S and YhmA-S was confirmed by immunoblot analysis using anti–S-tag antibody (Medical and Biological Laboratories, Nagoya, Japan) (Figure S3 in the supplemental material).

Construction of the Ptet-*ctpA-S* Δ*yhmA* strain. To control expression of the *ctpA* gene in the Δ*yhmA* background, we disrupted *yhmA* using the *bar* gene in the Ptet-*ctpA-S* strain. A gene disruption cassette encompassing 2 kb of the 5'-end of the *yhmA* gene, 1.8 kb of *bar*, and 2 kb of the 3'-end of the *yhmA* gene was constructed by

recombinant PCR using the primer pairs AKyhmA-FC/AKyhmA-bar-R1, AKymhA-bar-F2/AKyhmA-bar-R2, and AKyhmA-bar-F3/AKyhmA-RC, respectively. For amplification of the *bar* gene, a plasmid carrying *bar* (kindly provided by Prof. Michael J. Hynes, University of Melbourne, Australia) (57) was used as the template DNA. The resultant DNA fragment was amplified with the primers AKyhmA-F1 and AKyhmA-R3 and used to transform *A. kawachii* strain Ptet-*ctpA-S*, yielding the Ptet-*ctpA-S* Δ*yhmA* strain. Transformants were selected on M agar medium with glufosinate extracted from the herbicide Basta (Bayer Crop Science, Bayer Japan, Tokyo, Japan). Introduction of the *bar* gene into the target locus was confirmed by PCR using the primer pair AKyhmA-FC and AKyhmA-RC (Fig. S5E in the supplemental material).

Construction of strains expressing CtpA-GFP and YhmA-GFP. The plasmid pGS, which carries the *A. kawachii sC* gene (51), was used to construct the expression vector for CtpA-GFP and YhmA-GFP. The genes *ctpA* or *yhmA* (without stop codon) and *gfp* were amplified by PCR using the primer pairs pGS-xxxx-gfp-inf-F1/pGS-xxxx-gfp-inf-R1 and pGS-xxxx-gfp-inf-F2/pGS-gfp-inf-R (where 'xxxx' indicates ctpA or yhmA; Table S3 in the supplemental material). For amplification of *gfp*, pFNO3 (58) was used as the template DNA. The amplified fragments were cloned into the SalI site of pGS using an In-Fusion HD cloning kit (Takara Bio).

Fluorescence microscopy. Strains expressing CtpA-GFP or YhmA-GFP were cultured in M or CAP medium. After cultivation in M medium for 12 h or CAP medium from 14 to 20 h, MitoTracker Red CMXRos (Thermo Fisher Scientific, Waltham, MA) was added to the medium at a concentration of 500 nM and incubated for 40 min. After incubation, the mycelia were washed three times with fresh M or CAP medium and then

observed under a DMI6000B inverted-type fluorescent microscope (Leica Microsystems, Wetzlar, Germany). Image contrast was adjusted using LAS AF Lite software, version 2.3.0, build 5131 (Leica Microsystems).

Construction of the *yhm2* disruptant. The *yhm2* gene was disrupted in *S. cerevisiae* W303-1A by insertion of the *kanMX* gene. The disruption cassette was constructed by PCR using the primer pair SCyhm2-del-F and SCyhm2-del-R, which contained 45 bp of the 5'- and 3'-ends of *yhm2*, respectively (Table S3 in the supplemental material). For amplification of the *kanMX* gene, pUG6 (59) was used as the template DNA. Transformants were selected on YPD agar medium with 200 μg/ml of G418 (Nacalai Tesque, Kyoto, Japan).

Complementation of *YHM2* and *yhmA* in the *yhm2* disruptant. For the complementation test, we cloned *S. cerevisiae YHM2* and *A. kawachii yhmA* into plasmid YCplac22 carrying *TRP1* (60). Next, 0.6 kb of the 5'-end of *YHM2*, 0.9 kb of *YHM2*, and 0.1 kb of the 3'-end of *YHM2* were amplified by PCR using YCplac22-yhm2-inf-F and YCplac22-yhm2-inf-R. The amplicon was cloned into the SalI site of YCplac22, yielding YCplac22-*yhm2*.

Next, 0.6 kb of the 5'-end of *YHM2* and *yhmA* were amplified by PCR using the primer pairs YCplac22-yhm2-inf-F/YCplac22-yhmA-inf-R1 and YCplac22-yhmA-inf-F2/YCplac22-yhmA-inf-R2, respectively. For amplification of *yhmA* without the intron, *A. kawachii* cDNA was used as the template. The cDNA from *A. kawachii* was prepared using RNAiso Plus (Takara Bio) and reverse-transcription using SuperScript IV (Thermo Fisher Scientific). The amplified fragments were inserted into the SalI site of YCplac22, yielding YCplac22-*YHM2* and YCplac22-*yhmA*, respectively. An In-Fusion HD cloning kit (Takara Bio) was used for the cloning reactions. The resultant plasmids, YCplac22-*YHM2* and YCplac22-*yhmA*, were

560 transformed into the *S. cerevisiae* Δ*yhm2* strain, yielding Δ*yhm2* + *yhm2* and Δ*yhm2* +
561 *yhmA*, respectively. Transformants were selected on SC agar medium without
562 tryptophan.

563 **Purification of CtpA-S and YhmA-S.** A single-step purification method based on
564 S-tag and S-protein affinity (61) was employed for purification of S-tagged CtpA and
565 YhmA from the *A. kawachii* Ptet-*ctpA-S* and Ptet-*yhmA-S* strains, respectively. The
566 Ptet-*ctpA-S* and Ptet-*yhmA-S* strains were cultured in M medium containing 20 μg/ml
567 Dox with shaking (163 rpm) at 30°C for 36 h and then harvested by filtration. The
568 mycelia were ground to a powder using a mortar and pestle in the presence of liquid
569 nitrogen. A total of 1 g wet weight of powdered mycelia was dissolved in 13 ml of
570 ice-cold extraction buffer (25 mM HEPES [pH 6.8], 300 mM NaCl, 0.5% NP-40, 250
571 μg/ml phenylmethylsulfonyl fluoride [PMSF], cOmplete [EDTA-free protease inhibitor
572 cocktail, Roche, Basel, Switzerland]) and vigorously mixed using a vortexer. Cell debris
573 was removed by centrifugation at 1,000 × *g* at 4°C for 5 min. The resulting supernatant
574 was centrifuged at 18,800 × *g* at 4°C for 15 min. The supernatant was stirred for 2 h at
575 4°C. Then, S-protein agarose (Merck Millipore, Darmstadt, Germany) was added to the
576 supernatant, and the resulting mixture was gently mixed for 1 h at 4°C using a rotator.
577 S-protein agarose was collected by centrifugation at 500 × *g* for 5 min and then washed
578 once with extraction buffer (containing 0.2% NP-40, 50 μg/ml PMSF), followed by 5
579 washes using wash buffer (25 mM HEPES [pH 6.8], 300 mM NaCl, 20 μg/ml PMSF,
580 cOmplete [Roche]). CtpA-S and YhmA-S protein was eluted from the S-protein agarose
581 by mixing with elution buffer (25 mM HEPES [pH 6.8], 300 mM NaCl, 0.1% NP-40, 3
582 M $MgCl_2 \cdot 7H_2O$) and incubating at 37°C for 10 min. The eluted protein was desalted
583 using Vivacon 500 ultrafiltration units (Sartorius, Gottingen, Germany) with a >10 kDa
584 molecular weight cut-off membrane and washed with buffer (25 mM HEPES [pH 6.8],

585 300 mM NaCl, 0.1% NP-40) 5 times. The concentrations of CtpA-S and YhmA-S were
586 determined using a Qubit protein assay kit (Thermo Fisher Scientific). The purified
587 proteins were subjected to sodium dodecyl sulfate–polyacrylamide gel electrophoresis
588 (SDS-PAGE) to confirm purity (Fig. S2 in the supplemental material).

589 **Transporter assay.** YhmA-S or CtpA-S reconstituted proteoliposomes in the
590 presence or absence of internal substrate were prepared using a freeze/thaw sonication
591 procedure (62). Briefly, liposomal vesicles were prepared by probe-type sonication
592 using a Sonifier 250A (Branson Ultrasonics, Division of Emerson Japan, Kanagawa,
593 Japan) with 100 mg of L-α-phosphatidylcholine from egg yolk (Nacalai Tesque) in
594 buffer G (10 mM PIPES, 50 mM NaCl, and 1 mM organic acids [oxaloacetate,
595 succinate, cis-aconitate, citrate, 2-oxoglutarate, or malate]). Solubilized CtpA-S and
596 YhmA-S (500 ng of each) was added to 500 µl of liposomes and immediately frozen in
597 liquid nitrogen and then sonicated after melting. Extraliposomal substrate was removed
598 using Bio Spin 6 columns (Bio-Rad, Hercules, CA). To initiate the transport reaction, 1
599 mM [1,5-^{14}C]-citrate (18.5 kBq) (PerkinElmer, Waltham, MA) was added and incubated
600 at 37°C for 30 min. After the reaction, extraliposomal labeled and nonlabeled substrates
601 were removed using Bio Spin 6 columns (Bio-Rad). Intraliposomal radioactivity was
602 then measured using a Tri-Carb 2810TR liquid scintillation analyzer (PerkinElmer) after
603 mixing with Ultima Gold scintillation cocktail (PerkinElmer).

604 **Measurement of intracellular nicotinamide cofactor levels.** To determine the
605 intracellular levels of nicotinamide cofactors, conidia (2×10^7 cells) of *A. kawachii*
606 control, Δ*ctpA*, and Δ*yhmA* strains were inoculated into 100 ml of M medium and
607 pre-cultured with shaking (163 rpm) at 30°C for 36 h. The mycelia were then
608 transferred to 50 ml of CAP medium and further cultivated for 12 h. The mycelia were
609 collected and ground to a fine powder using a mortar and pestle in the presence of liquid

610 nitrogen. Next, 10 ml of cold PBS (1.37 M NaCl, 81 mM Na_2HPO_4, 26.8 mM KCl, 14.7
611 mM KH_2PO_4) was added to 1 g of mycelial powder, vortexed, and then centrifuged at
612 138,000 × *g* at 4°C for 30 min. The NADH/NAD^+ ratio, total amount of NADH and
613 NAD^+, NADPH/$NADP^+$ ratio, and total amount of NADPH and $NADP^+$ were measured
614 using an Amplite Fluorimetric NAD/NADH ratio assay kit (red fluorescence) and
615 Amplite Fluorimetric NADP/NADPH ratio assay kit (red fluorescence) (AAT Bioquest,
616 Sunnyvale, CA), respectively, according to the manufacturer's protocol. Fluorescence
617 was detected using an Infinite M200 FA (Tecan, Männedorf, Switzerland).

618 **Measurement of extracellular and intracellular organic acids.** To measure levels
619 of extracellular and intracellular organic acids, conidia (2×10^7 cells) of *A. kawachii*
620 control, Δ*ctpA*, Δ*yhmA* strains were inoculated into 100 ml of M medium and
621 pre-cultivated with shaking (180 rpm) at 30°C for 36 h and then transferred to 50 ml of
622 CAP medium and further cultivated with shaking (163 rpm) at 30°C for 48 h. The
623 Ptet-*ctpA-S* Δ*yhmA* strain was pre-cultured in M medium with 1 μg/ml Dox and
624 transferred to CAP medium without Dox. The culture supernatant was filtered through a
625 0.2-μm pore size PTFE filter (Toyo Roshi Kaisha, Japan) and used as the extracellular
626 fraction. Mycelia were used for preparation of the intracellular fraction using a hot
627 water extraction method (63), with modifications. After mycelial growth was measured
628 as wet weight, the mycelia were ground to a powder using a mortar and pestle in the
629 presence of liquid nitrogen. The mycelia were then dissolved in 10 ml of hot water
630 (80°C) per 1 g of mycelial powder, vortexed, and then centrifuged at 138,000 × *g* at 4°C
631 for 30 min. The supernatant was filtered through a 0.2-μm pore size filter and used as
632 the intracellular fraction.

633 The concentrations of organic acids in the extracellular and intracellular fractions
634 were determined using a Prominence HPLC system (Shimadzu, Kyoto, Japan) equipped

635 with a CDD-10AVP conductivity detector (Shimadzu). The organic acids were separated
636 using tandem Shimadzu Shim-pack SCR-102H columns (300 × 8 mm I.D., Shimadzu)
637 at 50°C using 4 mM *p*-toluenesulfonic acid monohydrate as the mobile phase at a flow
638 rate of 0.8 ml/min. The flow rate of the post-column reaction solution (4 mM
639 *p*-toluenesulfonic acid monohydrate, 16 mM bis-Tris, and 80 µM EDTA) was 0.8
640 ml/min.

641 **Measurement of intracellular amino acids.** Intracellular fractions of *A. kawachii*
642 strains were prepared as described above. Amino acids were analyzed using a
643 Prominence HPLC system (Shimadzu) equipped with a fluorescence detector
644 (RF-10AXL, Shimadzu) according to a post-column fluorescence derivatization method.
645 Separation of amino acids was achieved using a Shimadzu Shim-pack Amino-Na
646 column (100 × 6.0 mm I.D., Shimadzu) at 60°C and a flow rate of 0.6 ml/min using an
647 amino acid mobile phase kit, Na type (Shimadzu). The fluorescence detector was set to
648 excitation/emission wavelengths of 350/450 nm. The reaction reagents were taken from
649 the amino acid reaction kit (Shimadzu) and maintained at a flow rate of 0.2 ml/min.

650 **Transcription analysis.** For RNA extraction from mycelia, conidia (2×10^7 cells) of
651 *A. kawachii* control strain were inoculated into 100 ml of M medium and cultured for 24,
652 30, 36, 48, 60, and 72 h at 30°C. For RNA extraction from conidia, conidia (2×10^5)
653 were spread onto M agar medium and cultivated at 30°C for 5 days. After incubation,
654 mycelia and conidia were collected and ground to a powder in the presence of liquid
655 nitrogen. RNA was extracted using RNAiso Plus (Takara Bio) according to the
656 manufacturer's protocol and then quantified using a NonoDrop-8000 (Thermo Fisher
657 Scientific). cDNA was synthesized from total RNA using a PrimeScript Perfect
658 real-time reagent kit (Takara Bio) according to the manufacturer's protocol. Real-time
659 RT-PCR was performed using a Thermal Cycler Dice real-time system MRQ (Takara

660 Bio) with SYBR Premix Ex Taq II (Tli RNaseH Plus) (Takara Bio). The following
661 primer sets were used: AKyhmA-RT-F and AKyhmA-RT-R for *yhmA*, AKctpA-RT-F
662 and AKctpA-RT-R for *ctpA*, AKwetA-RT-F and AKwetA-RT-R for *wetA*, and
663 AKactA-RT-F and AKactA-RT-R for *actA* (Table S3 in the supplemental material).
664

665 **ACKNOWLEDGMENTS**

666 This study is supported in part by Yonemori Seishin Ikuseikai, Sasakawa Scientific
667 Research Grant from the Japan Science Society, Institute for Fermentation, Osaka (IFO),
668 and by a Grant-in-Aid for Scientific Research (C) (no. 16K07672). C. K. was supported
669 by a Grant-in-Aid for JSPS Research Fellows (no. 17J02753).
670

671 **REFERENCES**

672 1. Akiyama H. 2010. Sake: the essence of 2000 years of Japanese wisdom gained
673 from brewing alcoholic beverages from rice. Brewing Society of Japan, Tokyo,
674 Japan.
675
676 2. Kitamura Y, Kusumoto K, Oguma T, Nagai T, Furukawa S, Suzuki C, Satomi M,
677 Magariyama Y, Takamine K, Tamaki H. 2016. Ethnic fermented foods and alcoholic
678 beverages of Japan. p 193–236. *In* Tamang JP (ed), Ethnic fermented foods and
679 alcoholic beverages of Asia, Springer India, New Delhi, India.
680
681 3. Suganuma T, Fujita K, Kitahara K. 2007. Some distinguishable properties between
682 acid-stable and neutral types of alpha-amylases from acid-producing koji. J Biosci
683 Bioeng 104:353–362.
684
685 4. Yamada O, Takara R, Hamada R, Hayashi R, Tsukahara M, Mikami S. 2011.
686 Molecular biological researches of Kuro-Koji molds, their classification and safety.
687 J Biosci Bioeng 112:233–237.
688
689 5. Hong SB, Lee M, Kim DH, Varga J, Frisvad JC, Perrone G, Gomi K, Yamada O,
690 Machida M, Houbraken J, Samson RA. 2013. *Aspergillus luchuensis*, an
691 industrially important black *Aspergillus* in East Asia. PLoS One 8:e63769.
692
693 6. Hong SB, Yamada O, Samson RA. 2014. Taxonomic re-evaluation of black koji
694 molds. Appl Microbiol Biotechnol 98:555–561.
695

7. Karaffa L, Kubicek CP. 2003. *Aspergillus niger* citric acid accumulation: do we understand this well working black box? Appl Microbiol Biotechnol 61:189–196.

8. Magnuson JK, Lasure LL. 2004. Organic acid production by filamentous fungi, p 307–340. *In* Tkacz JS, Lange L (ed), Advances in fungal biotechnology for industry, agriculture, and medicine. Springer, Boston, MA.

9. Legisa M, Mattey M. 2007. Changes in primary metabolism leading to citric acid overflow in *Aspergillus niger*. Biotechnol Lett 29:181–190.

10. Jaklitsch WM, Kubicek CP, Scrutton MC. 1991. Intracellular organisation of citrate production in *Aspergillus niger*. Can J Microbiol 37:823–827.

11. Ruijter GJG, Panneman H, Xu D-B, Visser J. 2000. Properties of *Aspergillus niger* citrate synthase and effects of *citA* overexpression on citric acid production. FEMS Microbiol Lett 184:35–40.

12. Torres N. 1994a. Modelling approach to control of carbohydrate metabolism during citric acid accumulation by *Aspergillus niger*. I. Model definition and stability of the steady state. Biotechnol Bioeng 44:104–111.

13. Torres N. 1994b. Modelling approach to control of carbohydrate metabolism during citric acid accumulation by *Aspergillus niger*. II. Sensitivity analysis. Biotechnol Bioeng 44:112–118.

14. Alvarez-Vasquez F, González-Alcón C, Torres NV. 2000. Metabolism of citric acid production by *Aspergillus niger*: model definition, steady-state analysis and constrained optimization of citric acid production rate. Biotechnol Bioeng 70:82–108.

15. Palmieri F, Stipani I, Quagliariello E, Klingenberg M. 1972. Kinetic Study of the Tricarboxylate Carrier in Rat Liver Mitochondria. Eur. J. Biochem 26:587–594.

16. Bisaccia F, De Palma A, Palmieri F. 1989. Identification and purification of the tricarboxylate carrier from rat liver mitochondria. Biochim Biophys Acta. 977:171–176.

17. Kaplan RS, Mayor JA, Wood DO. 1993. The mitochondrial tricarboxylate transport protein. cDNA cloning, primary structure, and comparison with other mitochondrial transport proteins. J Biol Chem 268:13682–13690.

18. Kaplan RS, Mayor JA, Gremse DA, Wood DO. 1995. High level expression and characterization of the mitochondrial citrate transport protein from the yeast *Saccharomyces cerevisiae*. J Biol Chem 270:4108–4114.

19. Xu Y, Kakhniashvili DA, Gremse DA, Wood DO, Mayor JA, Walters DE, Kaplan RS. 2000. The yeast mitochondrial citrate transport protein. Probing the roles of cysteines, Arg(181), and Arg(189) in transporter function. J Biol Chem 275:7117–7124.

20. Watson JA, Lowenstein JM. 1970. Citrate and the conversion of carbohydrate into fat. Fatty acid synthesis by a combination of cytoplasm and mitochondria. J Biol Chem 245:5993–6002.

21. Brunengraber H, Lowenstein JM. 1973. Effect of (-)-hydroxycitrate on ethanol metabolism. FEBS Lett 36:130–132.

22. Endemann G, Goetz PG, Edmond J, Brunengraber H. 1982. Lipogenesis from ketone bodies in the isolated perfused rat liver. Evidence for the cytosolic activation of acetoacetate. J Biol Chem 257:3434–3440.

23. Conover TE. 1987. Does citrate transport supply both acetyl groups and NADPH for cytoplasmic fatty acid synthesis? Trends Biochem Sci 12:88–89.

24. Kaplan RS, Mayor JA, Kakhniashvili D, Gremse DA, Wood DO, Nelson DR. 1996. Deletion of the nuclear gene encoding the mitochondrial citrate transport protein from *Saccharomyces cerevisiae*. Biochem Biophys Res Commun 226:657–662.

25. Fernández M, Fernández E, Rodicio R. 1994 ACR1, a gene encoding a protein related to mitochondrial carriers, is essential for acetyl-CoA synthetase activity in *Saccharomyces cerevisiae*. Mol Gen Genet 242:727–735.

26. Palmieri L, Lasorsa FM, De Palma A, Palmieri F, Runswick MJ, Walker JE. 1997. Identification of the yeast ACR1 gene product as a succinate-fumarate transporter essential for growth on ethanol or acetate. FEBS Lett 417:114–118.

27. Palmieri L, Lasorsa FM, Vozza A, Agrimi G, Fiermonte G, Runswick MJ, Walker JE, Palmieri F. 2000. Identification and functions of new transporters in yeast mitochondria. Biochim Biophys Acta 1459:363–369.

28. Kirimura K, Kobayashi K, Ueda Y, Hattori T. 2016. Phenotypes of gene disruptants in relation to a putative mitochondrial malate-citrate shuttle protein in citric acid-producing *Aspergillus niger*. Biosci Biotechnol Biochem 80:1737–1746.

29. Futagami T, Mori K, Wada S, Ida H, Kajiwara Y, Takashita H, Tashiro K, Yamada O, Omori T, Kuhara S, Goto M. 2015. Transcriptomic analysis of temperature responses of *Aspergillus kawachii* during barley koji production. Appl Environ Microbiol 81:1353–1363.

30. Omori T, Takeshima N, Shimoda M. 1994. Formation of acid-labile α-amylase during barley-koji production. J Ferment Bioeng 78:27–30.

31. Castegna A, Scarcia P, Agrimi G, Palmieri L, Rottensteiner H, Spera I, Germinario L, Palmieri F. 2010. Identification and functional characterization of a novel mitochondrial carrier for citrate and oxoglutarate in *Saccharomyces cerevisiae*. J Biol Chem 285:17359–17370.

32. Cho JH, Ha SJ, Kao LR, Megraw TL, Chae CB. 1998. A novel DNA-binding protein bound to the mitochondrial inner membrane restores the null mutation of mitochondrial histone Abf2p in *Saccharomyces cerevisiae*. Mol Cell Biol 18:5712–

5723.

33. Saraste M, Walker JE. 1982. Internal sequence repeats and the path of polypeptide in mitochondrial ADP/ATP translocase. FEBS Lett 144:250–254.

34. Kunji ER. 2004. The role and structure of mitochondrial carriers. FEBS Letters 564:239–244.

35. Robinson AJ, Kunji ER. 2006. Mitochondrial carriers in the cytoplasmic state have a common substrate binding site. Proc Natl Acad Sci USA 103:2617–2622.

36. Ma C, Remani S, Sun J, Kotaria R, Mayor JA, Walters DE, Kaplan RS. 2007. Identification of the substrate binding sites within the yeast mitochondrial citrate transport protein. J Biol Chem 282:17210–17220.

37. Aluvila S, Kotaria R, Sun J, Mayor JA, Walters DE, Harrison DH, Kaplan RS. 2010. The yeast mitochondrial citrate transport protein: molecular determinants of its substrate specificity. J Biol Chem 285:27314–27326.

38. van Leeuwen MR, Krijgsheld P, Bleichrodt R, Menke H, Stam H, Stark J, Wösten HA, Dijksterhuis J. 2013. Germination of conidia of *Aspergillus niger* is accompanied by major changes in RNA profiles. Stud Mycol 74:59–70.

39. Ljungdahl PO, Daignan-Fornier B. 2012. Regulation of amino acid, nucleotide, and phosphate metabolism in *Saccharomyces cerevisiae*. Genetics 190:885–929.

40. Darby MM, Serebreni L, Pan X, Boeke JD, Corden JL. 2012. The *Saccharomyces cerevisiae* Nrd1-Nab3 transcription termination pathway acts in opposition to Ras signaling and mediates response to nutrient depletion. Mol Cell Biol 32:1762–1775.

41. Kaplan RS, Mayor JA, Johnston N, Oliveira DL. 1990. Purification and characterization of the reconstitutively active tricarboxylate transporter from rat liver mitochondria. J Biol Chem 265:13379–13385.

42. Pel HJ, de Winde JH, Archer DB, Dyer PS, Hofmann G, Schaap PJ, Turner G, de Vries RP, Albang R, Albermann K, Andersen MR, Bendtsen JD, Benen JA, van den Berg M, Breestraat S, Caddick MX, Contreras R, Cornell M, Coutinho PM, Danchin EG, Debets AJ, Dekker P, van Dijck PW, van Dijk A, Dijkhuizen L, Driessen AJ, d'Enfert C, Geysens S, Goosen C, Groot GS, de Groot PW, Guillemette T, Henrissat B, Herweijer M, van den Hombergh JP, van den Hondel CA, van der Heijden RT, van der Kaaij RM, Klis FM, Kools HJ, Kubicek CP, van Kuyk PA, Lauber J, Lu X, van der Maarel MJ, Meulenberg R, Menke H, Mortimer MA, Nielsen J, Oliver SG, Olsthoorn M, Pal K, van Peij NN, Ram AF, Rinas U, Roubos JA, Sagt CM, Schmoll M, Sun J, Ussery D, Varga J, Vervecken W, van de Vondervoort PJ, Wedler H, Wösten HA, Zeng AP, van Ooyen AJ, Visser J, Stam H. 2007. Genome sequencing and analysis of the versatile cell factory *Aspergillus niger* CBS 513.88. Nat Biotechnol 25:221–231.

43. Umbarger HE. 1978. Amino acid biosynthesis and its regulation. Annu Rev Biochem 47:532–606.

44. Bhattacharjee JK. 1985. alpha-Aminoadipate pathway for the biosynthesis of lysine in lower eukaryotes. Crit Rev Microbiol 12:131–151.

45. Garrad RC, Bhattacharjee JK. 1992. Lysine biosynthesis in selected pathogenic fungi: characterization of lysine auxotrophs and the cloned *LYS1* gene of *Candida albicans*. J Bacteriol 174:7379–7384.

46. Zabriskie TM, Jackson MD. 2000. Lysine biosynthesis and metabolism in fungi. Natural Product Reports 17:85–97.

47. Schöbel F, Jacobsen ID, Brock M. 2010. Evaluation of lysine biosynthesis as an antifungal drug target: biochemical characterization of *Aspergillus fumigatus* homocitrate synthase and virulence studies. Eukaryot Cell 9:878–893.

48. Fazius F, Shelest E, Gebhardt P, Brock M. 2012. The fungal α-aminoadipate pathway for lysine biosynthesis requires two enzymes of the aconitase family for the isomerization of homocitrate to homoisocitrate. Mol Microbiol 86:1508–1530.

49. Scarcia P, Palmieri L, Agrimi G, Palmieri F, Rottensteiner H. 2017. Three mitochondrial transporters of *Saccharomyces cerevisiae* are essential for ammonium fixation and lysine biosynthesis in synthetic minimal medium. Mol Genet Metab 122:54–60.

50. Palmieri L, Agrimi G, Runswick MJ, Fearnley IM, Palmieri F, Walker JE. 2001.

Identification in *Saccharomyces cerevisiae* of two isoforms of a novel mitochondrial transporter for 2-oxoadipate and 2-oxoglutarate. J Biol Chem 276:1916–1922.

51. Kadooka C, Onitsuka S, Uzawa M, Tashiro S, Kajiwara Y, Takashita H, Okutsu K, Yoshizaki Y, Takamine K, Goto M, Tamaki H, Futagami T. 2016. Marker recycling system using the sC gene in the white koji mold, *Aspergillus luchuensis* mut. *kawachii*. J Gen Appl Microbiol 62:160–163.

52. Wallis JW, Chrebet G, Brodsky G, Rolfe M, Rothstein R. 1989. A hyperrecombination mutation in *S. cerevisiae* identifies a novel eukaryotic topoisomerase. Cell 58: 409–419.

53. Barratt RW, Johnson GB, Ogata WN. 1965. Wild-type and mutant stocks of *Aspergillus nidulans*. Genetics 52:233–246.

54. Sherman F. 1991. Getting started with yeast. Methods Enzymol 194:3–21.

55. Aramayo R, Adams TH, Timberlake WE. 1989. A large cluster of highly expressed genes is dispensable for growth and development in *Aspergillus nidulans*. Genetics 122:65–71.

56. Meyer V, Wanka F, van Gent J, Arentshorst M, van den Hondel CA, Ram AF. 2011. Fungal gene expression on demand: an inducible, tunable, and metabolism-independent expression system for *Aspergillus niger*. Appl Environ

Microbiol 77:2975–2983.

57. Nayak T, Szewczyk E, Oakley CE, Osmani A, Ukil L, Murray SL, Hynes MJ, Osmani SA, Oakley BR. 2006. A versatile and efficient gene-targeting system for *Aspergillus nidulans*. Genetics 172:1557–1566.

58. Yang L, Ukil L, Osmani A, Nahm F, Davies J, De Souza CP, Dou X, Perez-Balaguer A, Osmani SA. 2004. Rapid production of gene replacement constructs and generation of a green fluorescent protein-tagged centromeric marker in *Aspergillus nidulans*. Eukaryot. Cell 3:1359–1362.

59. Güldener U, Heck S, Fielder T, Beinhauer J, Hegemann JH. 1996. A new efficient gene disruption cassette for repeated use in budding yeast. Nucleic Acids Res 24:2519–2524.

60. Dores MR, Schnell JD, Maldonado-Baez L, Wendland B, Hicke L. 2010. The function of yeast epsin and Ede1 ubiquitin-binding domains during receptor internalization. Traffic 11:151–160.

61. Liu HL, Osmani AH, Ukil L, Son S, Markossian S, Shen KF, Govindaraghavan M, Varadaraj A, Hashmi SB, De Souza CP, Osmani SA. 2010. Single-step affinity purification for fungal proteomics. Eukaryot Cell 9:831–833.

62. Palmieri F, Indiveri C, Bisaccia F, Iacobazzi V. 1995. Mitochondrial metabolite carrier proteins: purification, reconstitution, and transport studies. Methods

921 Enzymol 260:349–369.

922

923 63. Canelas AB, ten Pierick A, Ras C, Seifar RM, van Dam JC, van Gulik WM,
924 Heijnen JJ. 2009. Quantitative evaluation of intracellular metabolite extraction
925 techniques for yeast metabolomics. Anal Chem 81:7379–7389.

926

927

928

FIGURE LEGENDS

Figure 1. Citrate transport activity of (A) CtpA-S and (B) YhmA-S. CtpA-S or YhmA-S reconstituted proteoliposomes were preloaded with or without 1 mM internal substrate (oxaloacetate, succinate, *cis*-aconitate, citrate, 2-oxoglutarate, or malate). The exchange assay was initiated by adding 1 mM [^{14}C]-citrate (18.5 kBq) to the exterior of the proteoliposomes and terminated after 30 min. The mean and standard deviation were determined from the results of 3 independent measurements.

Figure 2. (A) Morphology of *A. kawachii* colonies. Conidia (10^4) were inoculated onto M agar medium and incubated for 4 days. (B) Conidia formation on M agar medium. Conidia (10^4) were inoculated onto M agar medium. After 5 days of incubation at 30°C, newly formed conidia were suspended in 0.01% (wt/vol) Tween 20 solution and counted using a hemocytometer. The mean and standard deviation of the number of conidia formed were determined from the results of 3 independently prepared agar plates. *, Statistically significant difference ($p < 0.05$, Welch's *t*-test) relative to the result for the control strain. (C) Colony formation of the *A. kawachii* Ptet-*ctpA-S* Δ*yhmA* strain. Conidia (10^4) were inoculated onto M agar medium with or without 1 μg/ml Dox and incubated at 30°C for 5 days. Scale bars indicate 1 cm.

Figure 3. (A) Extracellular and (B) intracellular organic acid production by *A. kawachii* strains. The control, Δ*ctpA*, Δ*yhmA*, and Ptet-*ctpA-S* Δ*yhmA* strains were pre-cultured in M medium for 36 h, then transferred to CAP medium and further cultivated for 48 h. The mean and standard deviation were determined from the results of 3 independent cultivations. *, Statistically significant difference ($p < 0.05$, Welch's *t*-test) relative to the result for the control strain.

954

955 **Figure 4.** (A) Growth curve of *A. kawachii* in M liquid medium at 30°C. (B)
956 Comparison of relative expression level of *wetA* in mycelia (stationary phase at 36 h)
957 and conidia. (C) Comparison of relative expression levels of *ctpA* and *yhmA* in mycelia
958 and conidia. (D) Comparison of relative expression levels of *ctpA* and *yhmA* in M
959 medium and CAP medium. All results were normalized to the expression level of the
960 actin-encoding gene, *actA*. The mean and standard deviation were determined from the
961 results of 3 independent cultivations. *, Statistically significant difference ($p < 0.05$,
962 Welch's *t*-test) relative to results obtained under other conditions.

963

964 **Figure 5.** (A) Expression of *ctpA-gfp* and *yhmA-gfp* complement the phenotypes of the
965 *A. kawachii* Δ*ctpA* and Δ*yhmA* strains, respectively. Control, Δ*ctpA*, and *ctpA-gfp* strains
966 were grown on M agar medium at 25°C, whereas the control, Δ*yhmA*, and *yhmA-gfp*
967 strains were grown on M agar medium at 30°C. Scale bars indicate 1 cm. Fluorescence
968 microscopic observation of (B) YhmA-GFP in M medium and (C) in CAP medium and
969 (D) CtpA-GFP in CAP medium. Scale bars indicate 10 μm.

970

971 **Figure 6.** Expression of *yhmA* complements the *S. cerevisiae* Δ*yhm2* phenotype.
972 Ten-fold serial dilutions of 10^7 cells of control strain, Δ*yhm2*, Δ*yhm2* + *yhm2*, and
973 Δ*yhm2* + *yhmA* cells (all strains pre-cultured for 24 h in SC medium without
974 tryptophan) were inoculated onto SD (glucose) or SA (acetate) medium and incubated at
975 30°C for 3 days.

976

977 **Figure 7.** Effect of amino acids on colony formation of the Ptet-*ctpA-S* Δ*yhmA* strain.
978 (A) Conidia (10^4) of the Ptet-*ctpA-S* Δ*yhmA* strain were inoculated onto M agar medium

979 with or without 1 μg/ml Dox and with 0.5% (wt/vol) various amino acids. (B) Conidia
980 (10^4) of the Ptet-*ctpA-S* Δ*yhmA* strain were grown on M agar medium with or without 1
981 μg/ml Dox and with 0.2~27 mM lysine. The conidia were incubated on the agar
982 medium at 30°C for 4 days. Scale bars indicate 1 cm.
983
984 **Figure 8.** Putative relationships between citrate transport, generation of NADPH, and
985 lysine biosynthesis in *A. kawachii*.
986

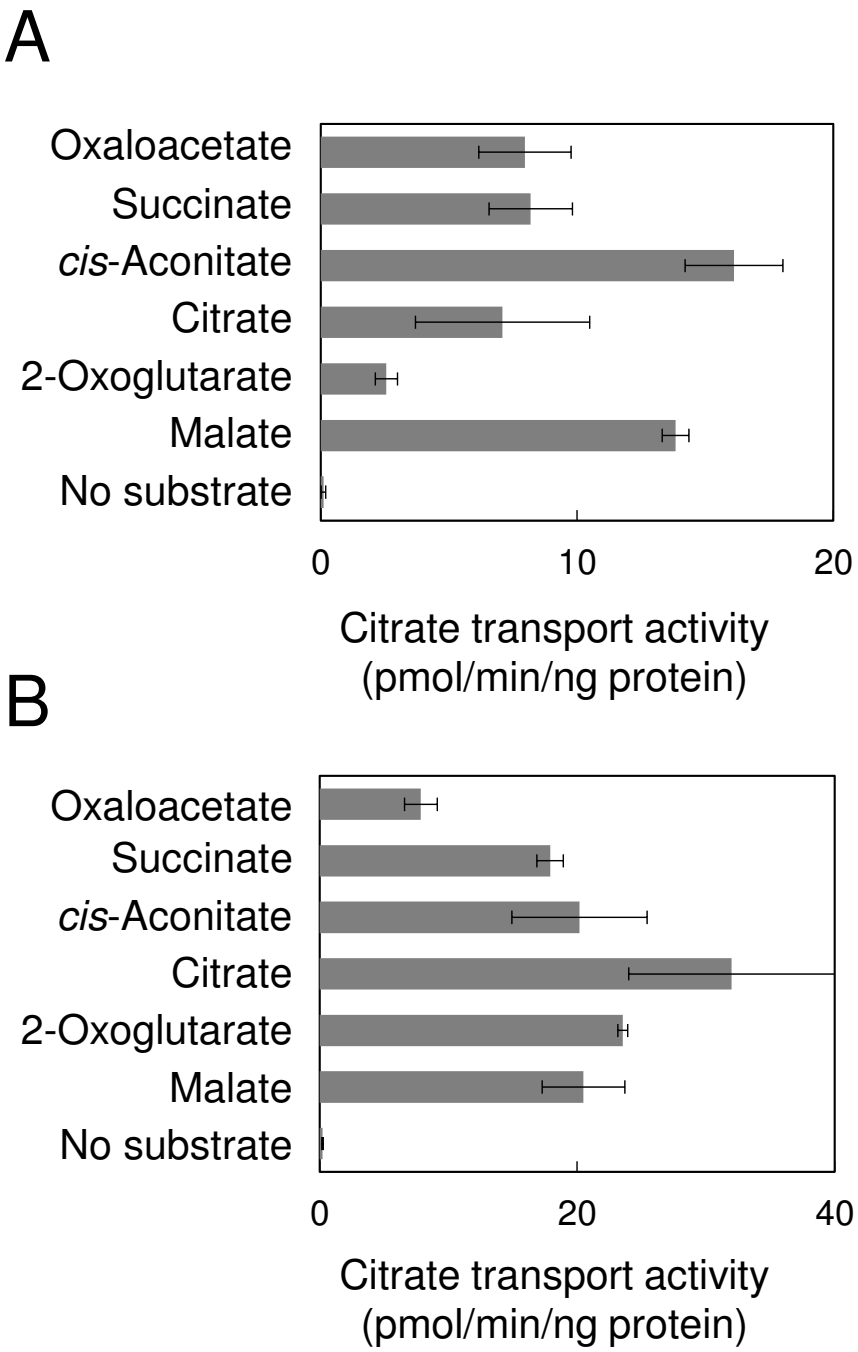

Figure 1. Citrate transport activity of (A) CtpA-S and (B) YhmA-S. CtpA-S or YhmA-S reconstituted proteoliposomes were preloaded with or without 1 mM internal substrate (oxaloacetate, succinate, *cis*-aconitate, citrate, 2-oxoglutarate, or malate). The exchange assay was initiated by adding 1 mM [^{14}C]-citrate (18.5 kBq) to the exterior of the proteoliposomes and terminated after 30 min. The mean and standard deviation were determined from the results of 3 independent measurements.

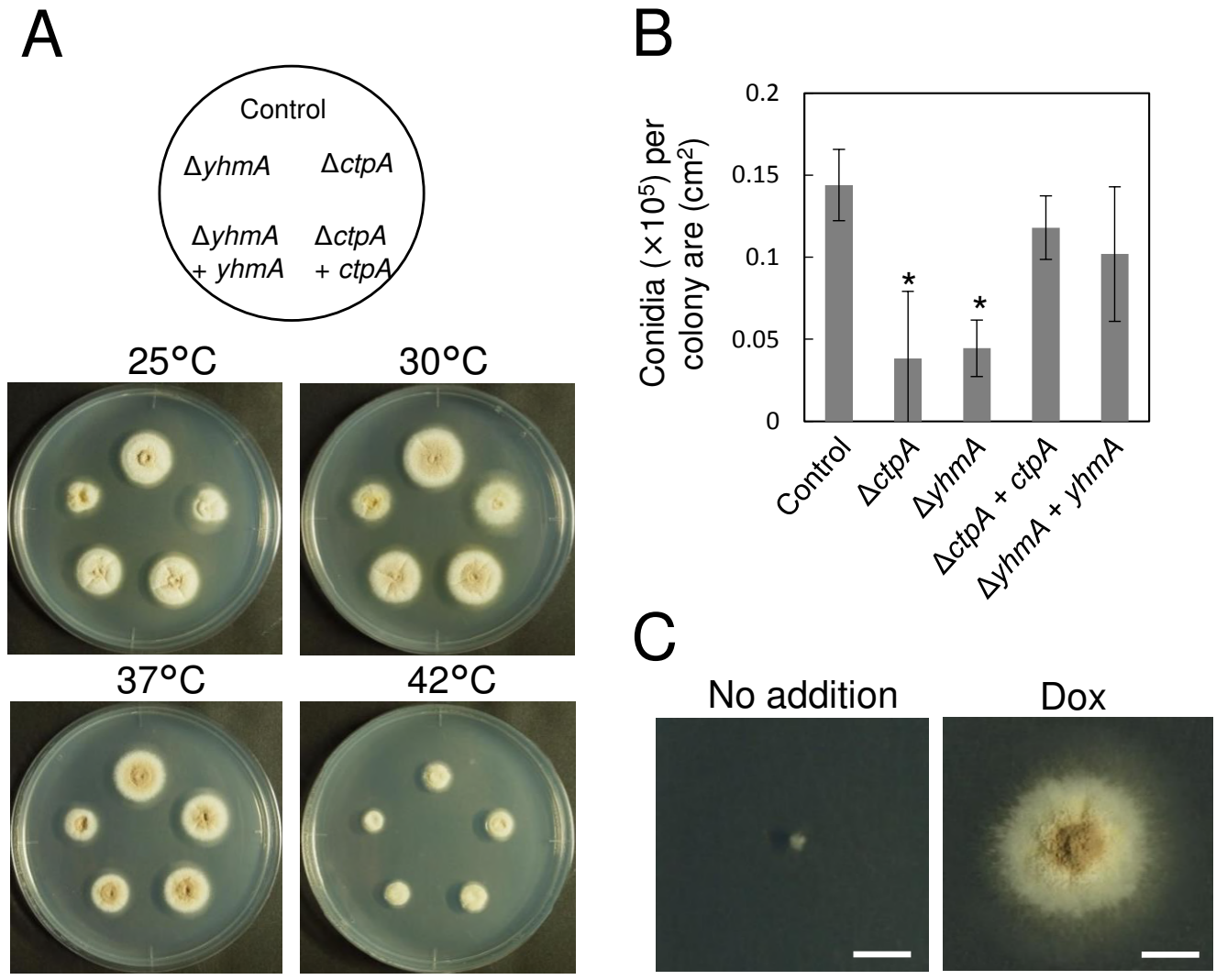

Figure 2. (A) Morphology of *A. kawachii* colonies. Conidia (10^4) were inoculated onto M agar medium and incubated for 4 days. (B) Conidia formation on M agar medium. Conidia (10^4) were inoculated onto M agar medium. After 5 days of incubation at 30° C, newly formed conidia were suspended in 0.01% (wt/vol) Tween 20 solution and counted using a hemocytometer. The mean and standard deviation of the number of conidia formed were determined from the results of 3 independently prepared agar plates. *, Statistically significant difference ($p < 0.05$, Welch's *t*-test) relative to the result for the control strain. (C) Colony formation of the *A. kawachii* Ptet-*ctpA-S* Δ*yhmA* strain. Conidia (10^4) were inoculated onto M agar medium with or without 1 μg/ml Dox and incubated at 30° C for 5 days. Scale bars indicate 1 cm.

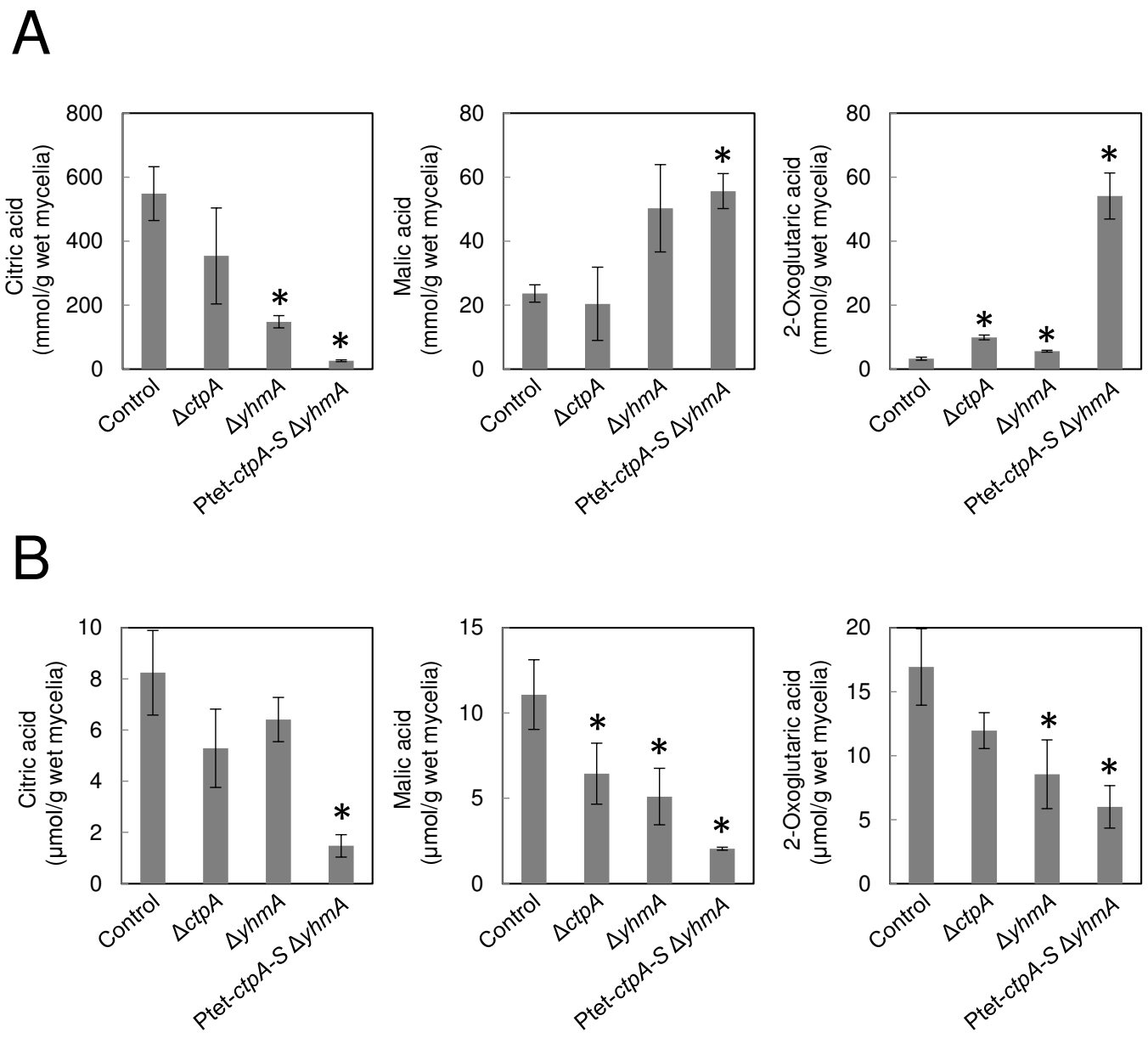

Figure 3. (A) Extracellular and (B) intracellular organic acid production by *A. kawachii* strains. The control, Δ*ctpA*, Δ*yhmA*, and Ptet-*ctpA-S* Δ*yhmA* strains were pre-cultured in M medium for 36 h, then transferred to CAP medium and further cultivated for 48 h. The mean and standard deviation were determined from the results of 3 independent cultivations. *, Statistically significant difference ($p < 0.05$, Welch's *t*-test) relative to the result for the control strain.

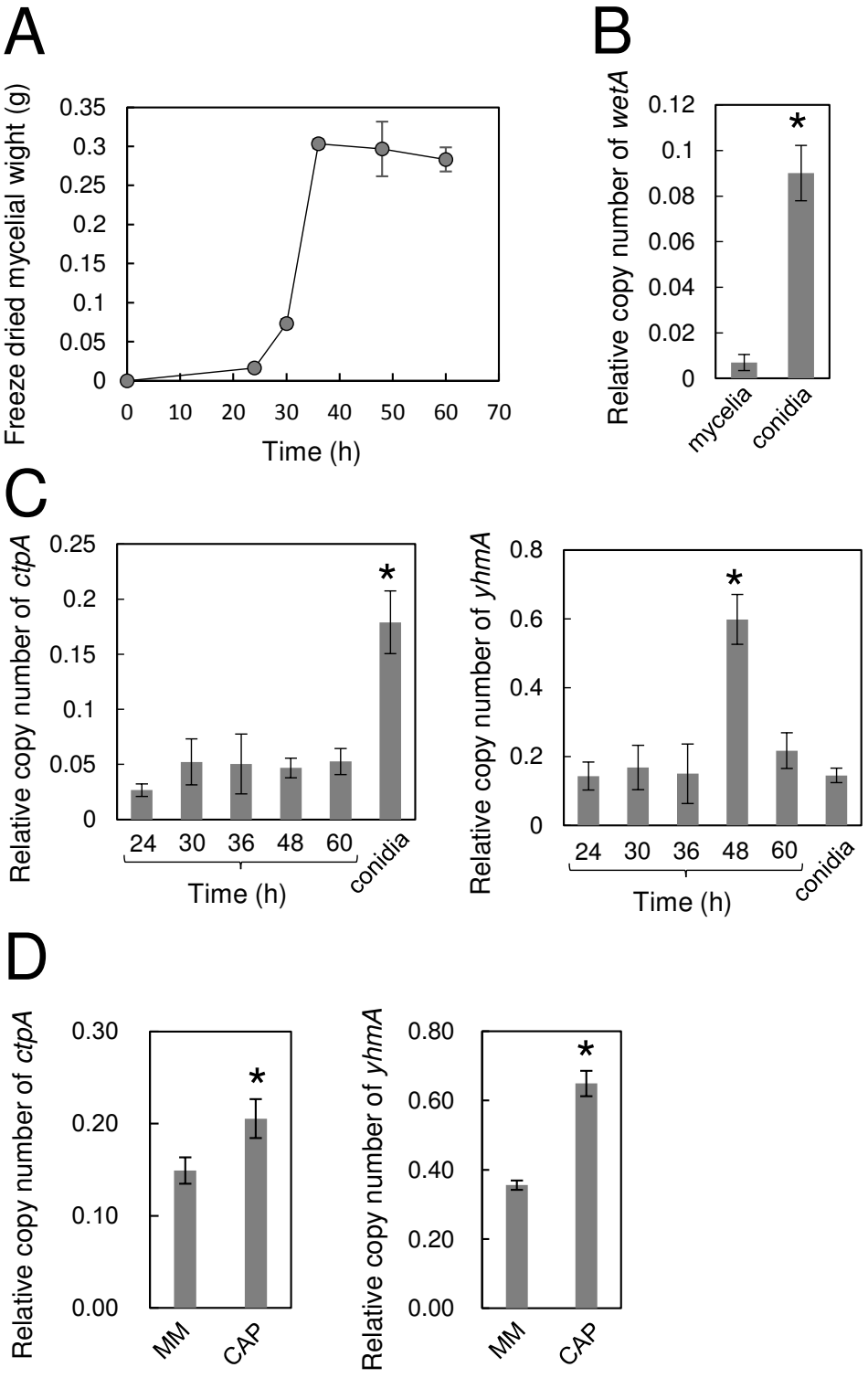

Figure 4. (A) Growth curve of *A. kawachii* in M liquid medium at 30° C. (B) Comparison of relative expression level of *wetA* in mycelia (stationary phase at 36 h) and conidia. (C) Comparison of relative expression levels of *ctpA* and *yhmA* in mycelia and conidia. (D) Comparison of relative expression levels of *ctpA* and *yhmA* in M medium and CAP medium. All results were normalized to the expression level of the actin-encoding gene, *actA*. The mean and standard deviation were determined from the results of 3 independent cultivations. *, Statistically significant difference ($p < 0.05$, Welch's *t*-test) relative to results obtained under other conditions.

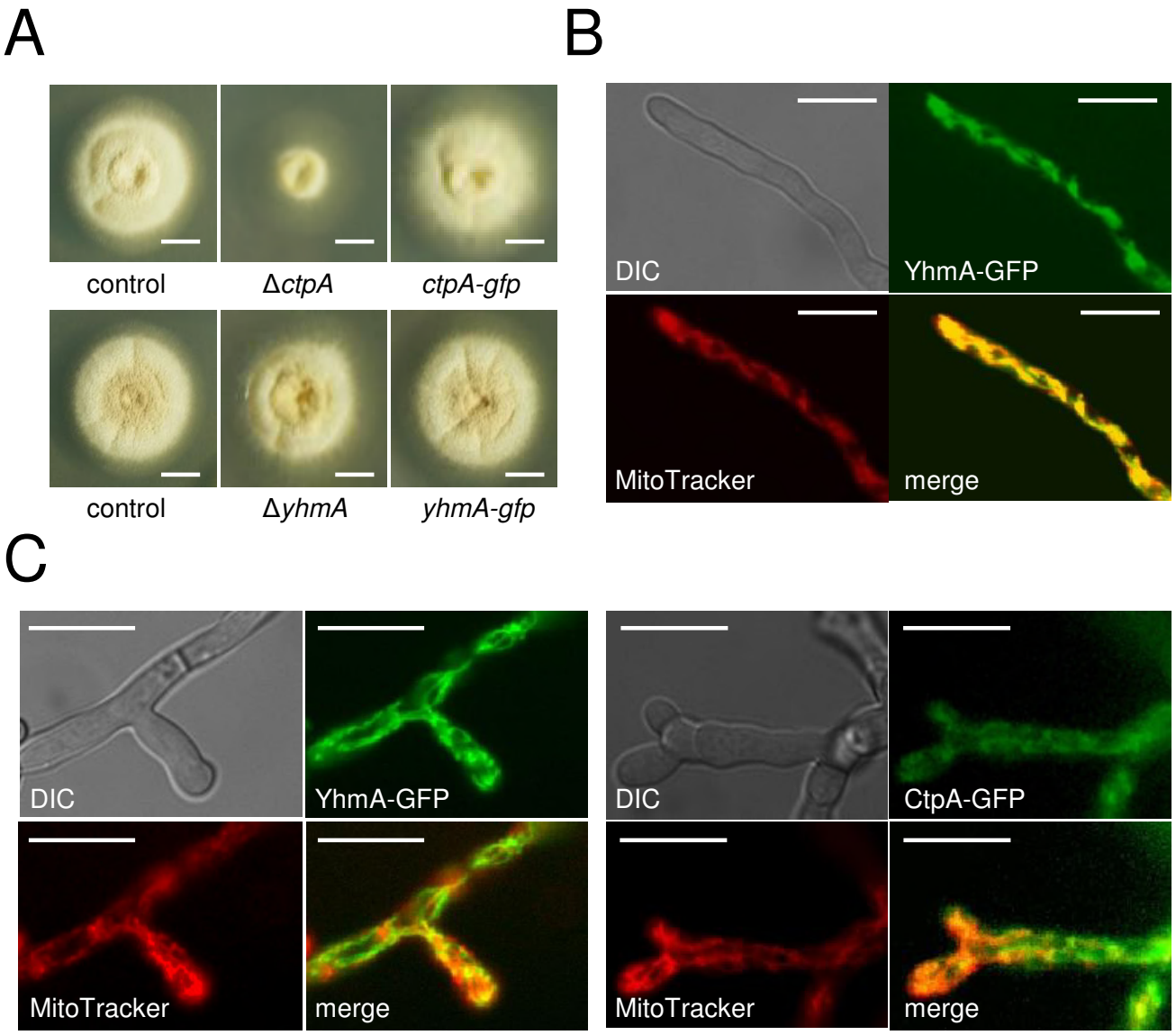

Figure 5. (A) Expression of *ctpA-gfp* and *yhmA-gfp* complement the phenotypes of the *A. kawachii* Δ*ctpA* and Δ*yhmA* strains, respectively. Control, Δ*ctpA*, and *ctpA-gfp* strains were grown on M agar medium at 25° C, whereas the control, Δ*yhmA*, and *yhmA-gfp* strains were grown on M agar medium at 30° C. Scale bars indicate 1 cm. Fluorescence microscopic observation of (B) YhmA-GFP in M medium and (C) in CAP medium and (D) CtpA-GFP in CAP medium. Scale bars indicate 10 μm.

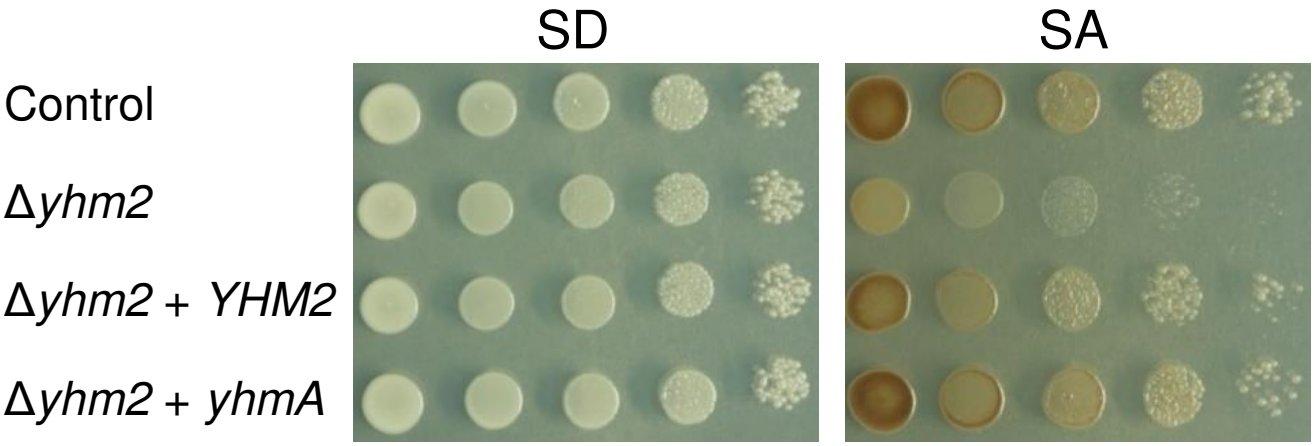

Figure 6. Expression of *yhmA* complements the *S. cerevisiae* Δ*yhm2* phenotype. Ten-fold serial dilutions of 10^7 cells of control strain, Δ*yhm2*, Δ*yhm2* + *yhm2*, and Δ*yhm2* + *yhmA* cells (all strains pre-cultured for 24 h in SC medium without tryptophan) were inoculated onto SD (glucose) or SA (acetate) medium and incubated at 30° C for 3 days.

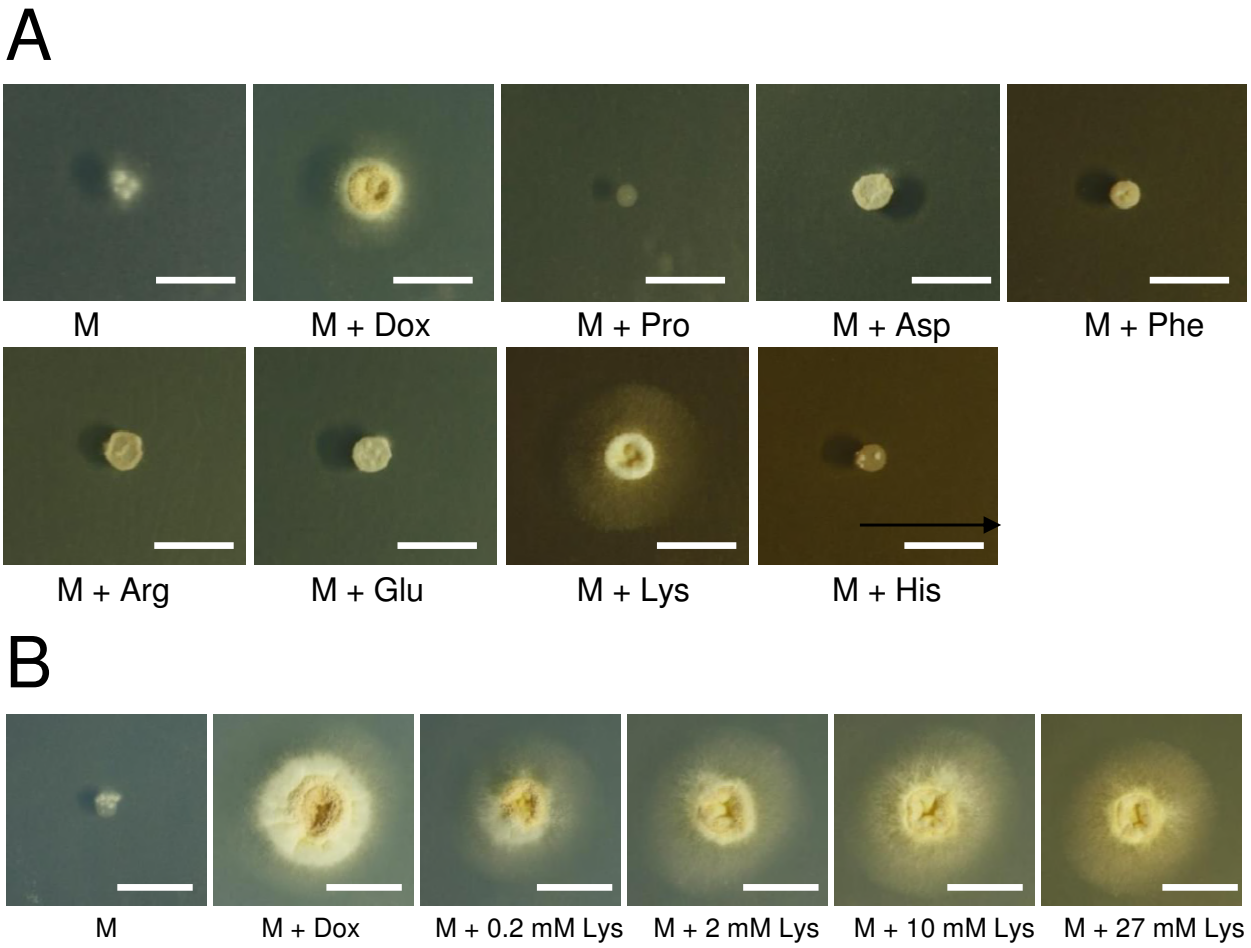

Figure 7. Effect of amino acids on colony formation of the Ptet-*ctpA-S* Δ*yhmA* strain. (A) Conidia (10^4) of the Ptet-*ctpA-S* Δ*yhmA* strain were inoculated onto M agar medium with or without 1 μg/ml Dox and with 0.5% (wt/vol) various amino acids. (B) Conidia (10^4) of the Ptet-*ctpA-S* Δ*yhmA* strain were grown on M agar medium with or without 1 μg/ml Dox and with 0.2~27 mM lysine. The conidia were incubated on the agar medium at 30° C for 4 days. Scale bars indicate 1 cm.

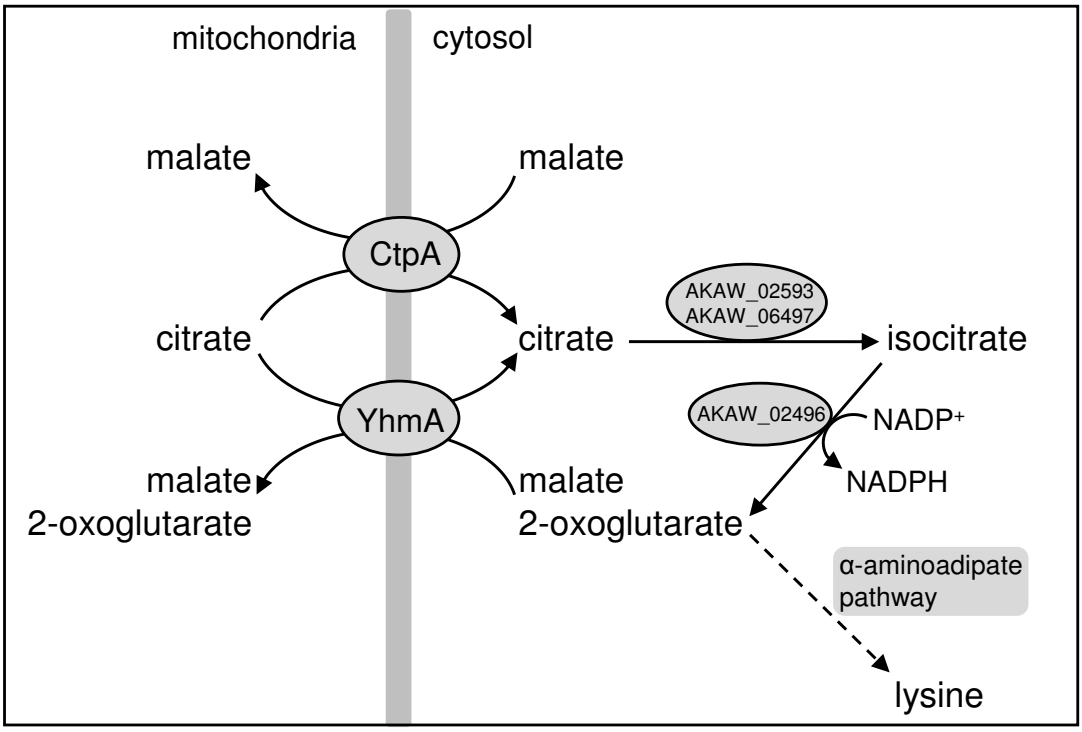

Figure 8. Putative relationships between citrate transport, generation of NADPH, and lysine biosynthesis in *A. kawachii*.

Table 1. Intracellular redox balance of *Aspergillus kawachii* strains.

Strain	$NADH/NAD^+$ ratio	$NADH + NAD^+$ (μmol/g wet cell)	$NADPH/NADP^+$ ratio	$NADPH + NADP^+$ (μmol/g wet cell)
Control	1.07 ± 0.21	4.49 ± 0.53	1.04 ± 0.0047	18.88 ± 0.96
Δ*ctpA*	0.98 ± 0.20	5.31 ± 0.14	1.43 ± 0.31	18.80 ± 1.62
Δ*yhmA*	1.17 ± 0.22	4.26 ± 0.23	0.55 ± 0.17*	22.64 ± 1.42

* Statistically significant difference ($p < 0.05$, Welch's t-test) relative to the result of control strain.

Table 2. Intracellular amino acid concentrations of *Aspergillus kawachii* strains.

Amino acids	Strains			
(μmol/g wet mycelia)	Control	Δ*ctpA*	Δ*yhmA*	Ptet-*ctpA-S* Δ*yhmA*
Asp	2.78 ± 0.47	1.85 ± 0.17	1.96 ± 0.083	1.19 ± 0.18*
Ser	2.87 ± 0.70	2.26 ± 0.14	2.69 ± 0.37	1.58 ± 0.18
Glu	7.37 ± 0.80	6.38 ± 0.92	7.63 ± 0.38	3.16 ± 0.80*
Gly	4.47 ± 1.06	4.41 ± 0.24	4.95 ± 0.74	1.55 ± 0.19*
Ala	39.49 ± 8.85	39.74 ± 2.25	43.26 ± 4.57	9.77 ± 0.78*
Ile	1.66 ± 0.96	1.07 ± 0.087	1.12 ± 0.076	0.24 ± 0.43
Leu	5.20 ± 0.26	2.82 ± 0.62	2.90 ± 0.35	1.67 ± 0.51
Tyr	3.05 ± 0.65	2.31 ± 0.19	2.33 ± 0.12	0.56 ± 0.98*
Phe	3.78 ± 0.73	2.991 ± 0.32	2.94 ± 0.18	2.22 ± 0.20
His	7.08 ± 0.99	4.71 ± 0.34	4.80 ± 0.14	3.58 ± 0.26*
Lys	11.30 ± 2.01	3.52 ± 1.03*	4.48 ± 0.52*	2.53 ± 0.82*
Arg	31.86 ± 9.33	19.06 ± 0.98	14.69 ± 0.46	11.55 ± 1.21
Met	0.70 ± 0.30	0.44 ± 0.08	0.38 ± 0.06	0.29 ± 0.13
Val	2.61 ± 0.63	1.91 ± 0.23	1.63 ± 0.24	0.84 ± 0.29*

* Statistically significant difference ($p < 0.05$, Welch's t-test) relative to the result of control strain.